DEFENCE R&D DÉFENSE

An Evaluation of the Watson-Watt And Butler Matrix Approaches For Direction Finding

William Read
Defence Research Establishment Ottawa

DEFENCE RESEARCH ESTABLISHMENT OTTAWA

TECHNICAL REPORT
DREO TR 1999-092
September 1999

National Defence Défense nationale

Canad

DEFENCE R&D DÉFENSE

An Evaluation of the Watson-Watt And Butler Matrix Approaches For Direction Finding

William Read
EW Sensors Group
Electronic Support Measures Section

DEFENCE RESEARCH ESTABLISHMENT OTTAWA

TECHNICAL REPORT
DREO TR 1999-092
September 1999

Project
5BB24

ABSTRACT

In this report, an evaluation of the Watson-Watt and Butler matrix approaches for tactical wideband radio direction finding applications is described. This evaluation was carried out using theoretical derivations and computer simulations, concentrating on the effects of various error mechanisms including internal noise, terrestrial and isotropic noise, cochannel interference, and multipath. A maximum likelihood (ML) approach was also derived and evaluated for comparative purposes to determine the accuracy trade-off between using an N-channel approach versus the three channel Watson-Watt approach and the two channel Butler matrix approach. The results indicate that the Watson-Watt approach is superior to the Butler matrix approach for current applications. In the future, this choice may need to be reassessed as lower cost receivers and faster processing equipment make more sophisticated approaches such as ML attractive alternatives.

RÉSUMÉ

Le présent résumé décrit l'évaluation des approches fondées sur Watson-Watt et la matrice de Butler pour les applications radiogoniométriques tactiques à large bande. L'évaluation a fait appel à des calculs théoriques et à des simulations par ordinateur portant sur les effets des divers mécanismes d'erreur, dont le bruit interne, le bruit terrestre et isotopique, l'interférence entre voies et la propagation par trajets multiples. L'évaluation a également permis de dériver et d'évaluer une approche baseé sur la probabilité maximale (PM) pour comparer les précisions angulaires obtenues en utilisant N canaux, les trois canaux de Watson-Watt et une matrice Butler à deux canaux. Les résultats montrent que l'approche de Watson-Watt est supérieure à la matrice de Butler pour les applications courantes. Dans l'avenir, on devra peut-être réévaluer ce choix, car les récepteurs peu coûteux et le matériel de traitement accéléré rendent plus intéressantes les approches poussées comme celles de la PM.

EXECUTIVE SUMMARY

Advances in technology have seen the development of improved communications receivers with larger and larger bandwidths. Coupled with advances in digital and computing technology, these new wideband receivers allow surveillance of spectral bands containing many communications signals with 100% detection of all transmissions in that band. The development of tactical wideband surveillance systems has also led to an interest in wideband radio direction finding (DF) with the ultimate goal of locating the source of transmission. To keep equipment size and cost to a minimum, DF approaches have been proposed which minimize the number of receiver channels by performing analog processing at the front end.

Two promising implementations for wideband DF are the Watson-Watt and the Butler matrix approaches. Although philosophically different, they have similar hardware and processing requirements. To evaluate and compare these two approaches theoretical derivations and computer simulations were carried out where the effects of noise, cochannel interference and multipath were present. Additionally, the performances of these two approaches were also compared with a more optimum maximum likelihood (ML) approach to determine the accuracy penalty incurred by reducing the number of receiver channels (the ML approach requires one receiver for every antenna).

For the theoretical evaluations of the Watson-Watt and Butler matrix approaches, four and eight-element circular antenna arrays were considered. It was found that when adjusting the size of these arrays, two critical antenna array radii exist where the gains of one or more of the receiver channels becomes zero leading to large bearing errors when noise or other types of interference are present. The smallest radius (approximately one-third the signal wavelength) at which this happens corresponds to zero gain in the reference channel (a channel common to both approaches and used for phase reference purposes). The problem can be overcome by using a central antenna for the reference instead of deriving it from the antennas in the circular array, although this could be difficult to do if a supporting mast occupies the central position. The second critical radius (approximately one-half the signal wavelength or slightly more) corresponds to the gain in the other channels going to zero, and there is no simple solution. Hence the maximum size is limited by this second critical radius. For a fixed array size, the upper frequency is limited accordingly. The ML approach is also limited by the same critical radii for the four-element array but not for the eight-element array which is capable of working up to an array radius of slightly less than three-quarters of the signal wavelength for an

eight-element antenna array with a correspondingly higher upper frequency limit.

In practical applications, external effects such as terrestrial and cosmic noise, cochannel interference, and multipath will be the dominant source of error. Under these conditions, the accuracies of both the Watson-Watt and Butler matrix approaches were determined to be relatively constant as the array size was increased (or equivalently as the frequency was increased) except close to the critical values (discussed in the previous paragraph) where accuracy rapidly degraded. There was relatively little improvement in either of the two approaches when an eight-element antenna array was used compared to a four-element array. Quantitatively, the Watson-Watt approach was found to be twice as accurate (i.e. one half the RMS bearing errors) as the Butler matrix approach. In comparison, the ML approach was significantly better with the best accuracy achieved using the eight-element array (upwards of five times better than the Watson-Watt approach).

Generally the results show that neither the Watson-Watt nor Butler matrix approaches achieve optimum accuracy under practical conditions and that utilizing more channels provides better accuracy. However, for a system where other constraints besides accuracy are important, such as low cost and realtime capability, and given the current economic climate and technological advances, the Watson-Watt approach is the best choice. The ML approach, although generally having better accuracy and a greater frequency range of operation, is considerably more expensive due to the greater number of receivers and the processing requirements. In the future, however, this choice may need to be reassessed as lower cost receivers and faster processing equipment make the ML approach a more attractive alternative.

TABLE OF CONTENTS

	Page
ABSTRACT/RÉSUMÉ	iii
EXECUTIVE SUMMARY	v
TABLE OF CONTENTS	vii
LIST OF FIGURES	ix
1.0 INTRODUCTION	1
2.0 DF THEORY	2
2.1 The Watson-Watt Approach	8
2.1.1 Four Element Array	8
2.1.2 Eight Element Array	11
2.2 The Butler Matrix Approach	14
2.2.1 Four Element Array	15
2.2.2 Eight Element Array	16
2.3 The Single Signal Maximum Likelihood Approach	18
3.0 ERRORS DUE TO NOISE AND INTERFERENCE	21
3.1 The Effect of Internal Noise	23
3.1.1 Internal Noise and the Watson-Watt Approach	24
3.1.2 Internal Noise and the Butler Matrix Approach	29
3.1.3 Internal Noise and Comparisons with Maximum Likelihood Performance	34
3.2 The Effect of External Interference	37
3.2.1 Interference and the Watson-Watt Approach	38
3.2.2 Interference and the Butler Matrix Approach	45
3.2.3 Interference and Comparisons with Maximum Likelihood Performance	51
4.0 CONCLUSIONS AND RECOMMENDATIONS	56
REFERENCES	59

LIST OF FIGURES

		Page
Figure 1:	Antenna geometry of a four-element circular array	3
Figure 2:	Antenna geometry of an eight-element circular array	4
Figure 3:	Values of β for a four-element circular array	6
Figure 4:	Values of β for an eight-element circular array	6
Figure 5:	Watson-Watt antenna patterns	8
Figure 6:	Adcock antenna setup for a four-element array	9
Figure 7:	Bias errors of a Watson-Watt system using a four-element array . .	11
Figure 8:	Adcock antenna setup for an eight-element array	11
Figure 9:	Bias error of a Watson-Watt system using an eight-element array . .	13
Figure 10:	Phase response of a circular array	14
Figure 11:	Bias error of a Butler matrix system using an eight-element array .	18
Figure 12:	Effect of the internal noise level on the performance of the Watson-Watt approach	27
Figure 13:	Effect of array radius on the performance of the Watson-Watt approach	28
Figure 14:	Effect of the internal noise level on the performance of the Butler matrix approach	31
Figure 15:	Effect of array radius on the performance of the Butler matrix approach	33
Figure 16:	Effect of external noise on different DF approach	35
Figure 17:	Effect of array radius on the performance of difference DF approach in the presence of internal noise	36
Figure 18:	Effect of external terrestrial interference on the Watson-Watt approach	41
Figure 19:	Effect of array radius on the performance of the Watson-Watt approach with external terrestrial interference	42

Figure 20: Effect of external isotropic noise on the Watson-Watt approach . . . 44

Figure 21: Effect of array radius on the performance of the Watson-Watt approach with external isotropic noise 45

Figure 22: Effect of external terrestrial interference on the Butler matrix approach 48

Figure 23: Effect of array radius on the performance of the Butler matrix approach with external terrestrial interference 49

Figure 24: Effect of external isotropic noise on the Butler matrix approach . . . 50

Figure 25: Effect of array radius on the performance of the Butler matrix approach with external isotropic noise 51

Figure 26: Effect of external noise on different DF approach 53

Figure 27: Effect of array radius on the performance of difference DF approach with external isotropic noise 54

Figure 28: Effect of external isotropic noise on different DF approach 55

Figure 29: Effect of array radius on the performance of difference DF approach with external isotropic noise 55

1.0 INTRODUCTION

Advances in technology have seen the development of improved communications receivers with larger and larger bandwidths. Coupled with advances in digital and computing technology, these new wideband receivers allow surveillance of spectral bands containing many communications signals with 100% detection of all transmissions in that band – something that was not possible previously. Once detected, these signals may then be demodulated and analyzed as necessary.

The development of tactical wideband surveillance systems has also led to an interest in wideband radio direction finding (DF) with the ultimate goal of locating the source of transmission. To keep equipment size and cost to a minimum, DF approaches have been proposed which minimize the number of receiver channels by performing analog processing at the front end. The front end processing, however, leads to compromises in performance since there is less flexibility in terms of how the received antenna signals are processed.

Two approaches to wideband DF, which appear to have the desired qualities, are the Watson-Watt approach and the Butler matrix approach. Although philosophically different approaches, their hardware implementation is similar and one might expect that the performance of both approaches would also be similar. However, subtle differences in approaches can often lead to unexpected and undesired consequences in terms of performance which is not something one wishes to discover after the equipment has been built. To address these concerns, and identify the more promising approach, an evaluation of these two approaches was carried out through theoretical derivations and computer simulations. This evaluation included the effects of noise, cochannel interference and multipath. Additionally, the performance of the Watson-Watt and Butler matrix approaches was compared with a more optimum maximum likelihood approach to highlight the performance trade-off being made.

This introduction is followed by a theoretical derivation of the Watson-Watt approach, the Butler matrix approach, and the maximum likelihood (ML) approach in Section 2. This is, in turn, followed by an evaluation of the theoretical and simulated susceptibility of the proposed wideband approaches to internal noise and external interference (including noise, cochannel interference, and multipath) in Section 3. The simulated susceptibility of the ML approach is also included for comparison. Finally, the conclusions and recommendations are presented in Section 5.

2.0 DF THEORY

For the purposes of this report only four and eight-element equally spaced circular antenna arrays are considered. This does not mean that the Watson-Watt or Butler matrix approaches are restricted to only these two antenna arrays, rather it provides a convenient basis for comparison and these are commonly used arrays for tactical DF applications.

Since none of the DF approaches discussed are capable of dealing with more than one signal at a time, it is assumed that the receiver outputs are digitized then processed using narrowband digital filters or FFT processing to separated the various signals before DF processing. Regardless of how a target signal has been isolated, the input to the DF processor is assumed to be a single complex sample from each channel at a sampling rate considerably lower than the sampling rate of the receivers (which is related to the difference in the receiver bandwidth and the signal bandwidth).

Averaging of the estimated signal bearing may also be done to produce a more stable estimate, however, this is not discussed in this report. Rather it is assumed that if the bearing errors have a random temporal component the error distribution will be Gaussian and averaging will then reduce the temporal RMS error by a factor of $1/\sqrt{K}$ where K is the number of bearings averaged. Note that in some instances, such as with multipath at the receiver site, the resultant error does not change over time so that averaging provides no improvement.

To maintain consistency in the derivations, the positions $(\mathrm{x}_n, \mathrm{y}_n)$ for $n = 0, 1, ..., N-1$ of the N antennas used in the circular arrays are defined according to

$$\mathrm{x}_n = r\cos\left(\frac{2\pi n}{N} + \vartheta\right) \tag{1}$$

$$\mathrm{y}_n = r\sin\left(\frac{2\pi n}{N} + \vartheta\right) \tag{2}$$

where the array has radius r, the origin is the center of the array, and ϑ gives the angle of the radial running through antenna 0 measured counter-clockwise from the X-axis (the array orientation). Figures 1 and 2 show the antenna positions graphically. The response of antenna n for a signal arriving from the direction ϕ (measured in the clockwise direction

from the y-axis) is then given by

$$x_n = s e^{j\frac{2\pi}{\lambda}(x_n \sin\phi + y_n \cos\phi)}$$

$$= s e^{j\frac{2\pi r}{\lambda}\sin\left(\phi + \frac{2\pi n}{N} + \vartheta\right)} \tag{3}$$

where s is the time dependent complex amplitude of the signal measured at the center of the antenna array, and λ is the signal wavelength.

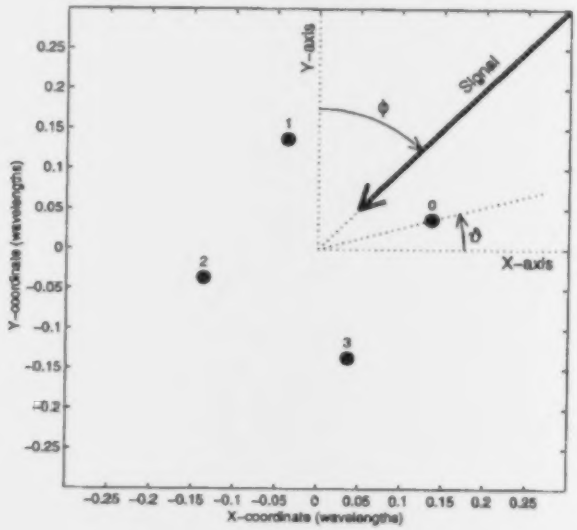

Figure 1: Geometry of a four-element circular array showing antenna positions (large dots) and orientation $\vartheta = 15°$, as well as signal direction $\phi = 45°$ (where the signal is represented by the large arrow).

Before continuing on to the detailed derivation of either the Watson-Watt approach or the Butler matrix approach, it is useful to consider some of the common features. Both approaches involve estimation of the signal direction using the equation

$$\hat{\phi} = \arctan\left(\frac{A}{B}\right) \tag{4}$$

where A and B are real-valued and the four quadrant version of the arctangent function is used (i.e., the signs of A and B are utilized to resolve the 180° ambiguity between the

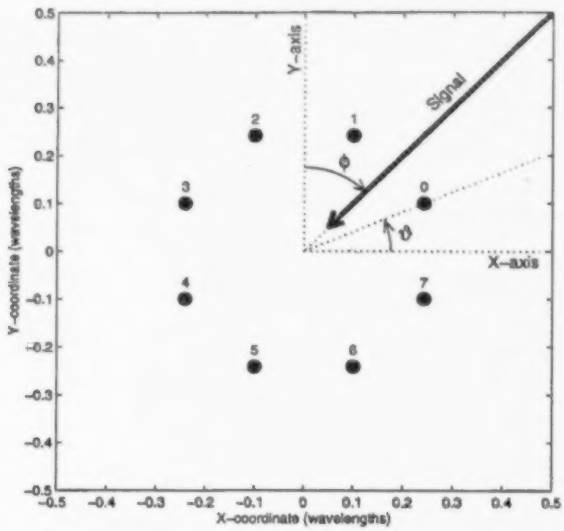

Figure 2: Geometry of a eight-element circular array showing antenna positions (large dots) and orientation $\vartheta = 22.5°$, as well as signal direction $\phi = 45°$ (where the signal is represented by the large arrow).

quantities $\frac{A}{B}$ and $\frac{-A}{-B}$). The four quadrant arctangent function also has the property

$$\hat{\phi} \;=\; \arctan\left(\frac{cA}{cB}\right) \tag{5}$$

where c is a positive real value.

In determining the signs of the quantities A and B, a reference channel is required. This channel is usually generated by summing the outputs from all the antennas in the array. The result is given by

$$\begin{aligned} v_{ref} &= \sum_{n=0}^{N-1} x_n \\ &= \sum_{n=0}^{N/2-1} x_n + x_{n+N/2} \\ &= \sum_{n=0}^{N/2-1} s e^{j\frac{2\pi r}{\lambda}\sin(\phi+\frac{2\pi n}{N}+\vartheta)} + s e^{j\frac{2\pi r}{\lambda}\sin(\phi+\frac{2\pi n}{N}+\pi+\vartheta)} \\ &= 2s\sum_{n=0}^{N/2-1} \cos\left(\frac{2\pi r}{\lambda}\sin(\phi+\frac{2\pi n}{N}+\vartheta)\right) \end{aligned}$$

$$= 2s\beta \tag{6}$$

where β is a real scaling factor. The value of β changes significantly with r, the radius of the antenna array, as shown in Figures 3 and 4, and is relatively independent of the signal direction ϕ except for values of $r > 0.3\lambda$ in the four element case. From these figures, the minimum value of β occurs for $\phi + \vartheta = (2k+1)\pi/N$ for $k = 0, ..., N-1$ and is given by

$$\beta_{min} = \begin{cases} 2\cos\left(\frac{\pi r\sqrt{2}}{\lambda}\right) & \text{for } N = 4 \\ 2\cos\left(\frac{2\pi r}{\lambda}\cos\frac{3\pi}{8}\right) + 2\cos\left(\frac{2\pi r}{\lambda}\cos\frac{\pi}{8}\right) & \text{for } N = 8 \end{cases} \tag{7}$$

Similarly, the maximum value of β occurs for $\phi + \vartheta = 2k\pi/N$ for $k = 0, ..., N-1$ and is given by

$$\beta_{max} = \begin{cases} 1 + \cos\left(\frac{2\pi r}{\lambda}\right) & \text{for } N = 4 \\ 1 + 2\cos\left(\frac{\pi r\sqrt{2}}{\lambda}\right) + \cos\left(\frac{2\pi r}{\lambda}\right) & \text{for } N = 8 \end{cases} \tag{8}$$

Alternatively, for the Watson-Watt approach, the reference can be obtained from the output of a single antenna placed at the center of the array. The reference output in this case is simply

$$v_{ref} = s \tag{9}$$

The advantage of using a single antenna is that it does not suffer from the zero problem associated with the summed output. The disadvantages are that an extra antenna and associated hardware are required and the central position of the array will typically be occupied by the mast used to support the antenna array. Hence, when discussing the reference voltage, the form given by (6) is assumed unless otherwise stated.

In Figures 3 and 4, β goes to zero then becomes negative for larger values of r. Since this is an undesirable condition (particularly $\beta = 0$), a suitable limit on r can be

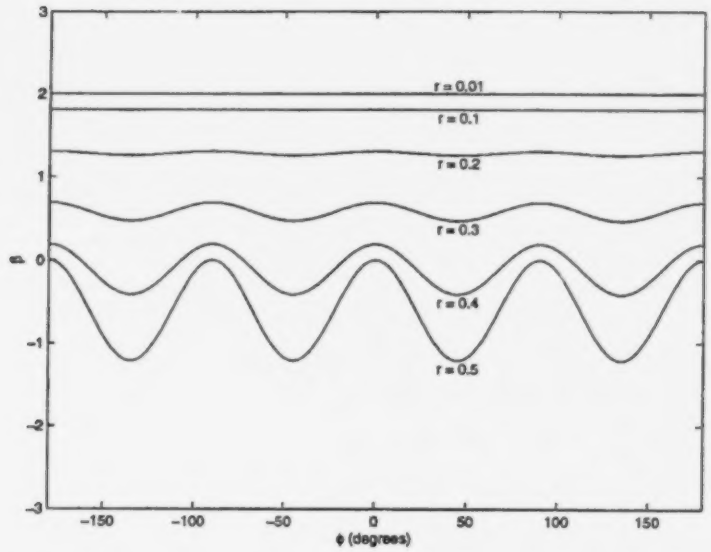

Figure 3: Value of β as a function of both the signal bearing and the radius of a four-element circular antenna array ($\vartheta = 0°$).

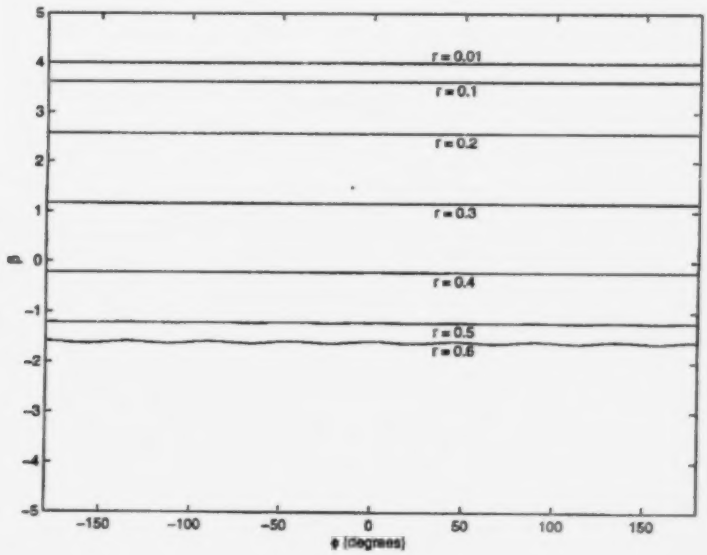

Figure 4: Value of β as a function of both the signal bearing and the radius of an eight-element circular antenna array ($\vartheta = 0°$).

determined by requiring that $\beta_{min} > 0$ which leads to

$$r_{max_0} = \begin{cases} \dfrac{\lambda}{2\sqrt{2}} & \text{for } N = 4 \\ \dfrac{\lambda}{2\sqrt{2}\cos\frac{\pi}{8}} & \text{for } N = 8 \end{cases} \tag{10}$$

These limitations on r only apply when the reference voltage is generated using the summed antenna outputs. For the central reference antenna approach there is no such limitation.

It is also useful to evaluate the term $x_n - x_{n+N/2}$ which figures prominently in generating the channel outputs for both approaches. Hence

$$\begin{aligned} x_n - x_{n+N/2} &= se^{j\frac{2\pi r}{\lambda}\sin\left(\phi+\frac{2\pi n}{N}+\vartheta\right)} - se^{j\frac{2\pi r}{\lambda}\sin\left(\phi+\frac{2\pi(n+N/2)}{N}+\vartheta\right)} \\ &= se^{j\frac{2\pi r}{\lambda}\sin\left(\phi+\frac{2\pi n}{N}+\vartheta\right)} - se^{j\frac{2\pi r}{\lambda}\sin\left(\phi+\frac{2\pi n}{N}+\pi+\vartheta\right)} \\ &= se^{j\frac{2\pi r}{\lambda}\sin\left(\phi+\frac{2\pi n}{N}\right)} - se^{-j\frac{2\pi r}{\lambda}\sin\left(\phi+\frac{2\pi n}{N}+\vartheta\right)} \\ &= j2s\sin\left(\frac{2\pi r}{\lambda}\sin(\phi+\frac{2\pi n}{N}+\vartheta)\right) \end{aligned} \tag{11}$$

Finally, some comments on mutual coupling effects are in order. Given the small spacings between antennas used in the antenna arrays discussed in this study (less than a wavelength), mutual coupling effects would be expected to figure prominently in the results. However it was found through simulation that, although mutual coupling does significantly affect channel gains and phases, the effects could be minimized through channel calibration with the result that performance was not appreciably different than when mutual coupling was absent. For example, assuming half-wave dipole elements and using the approach discussed in [1] to model mutual coupling, the summed reference voltage amplitude was reduced by a factor ranging from N (for $r \to 0$) to 1 (for $r \to r_{max_0}$). The value of r_{max_0} was not significantly changed, however, and the phase offset was easily corrected, minimizing the degradation of the reference voltage (the reduction in amplitude was minimal for values of r where bearing estimation could have been compromised). Hence to avoid unnecessarily complicating the derivation and evaluation of the direction

finding approaches discussed in this report, mutual coupling effects were ignored.

2.1 The Watson-Watt Approach

The Watson-Watt approach uses two orthogonal directional antennas with the gain pattern of one antenna given by

$$g_{EW}(\phi) = \sin\phi \tag{12}$$

and the gain of the second antenna given by

$$g_{NS}(\phi) = \cos\phi \tag{13}$$

where in this discussion the gains are real valued but may be positive or negative. If these two gain values are measured for a given signal, as shown in Figure 5, then the signal bearing can be estimated using

$$\hat{\phi} = \arctan\left(\frac{g_{EW}(\phi)}{g_{NS}(\phi)}\right) \tag{14}$$

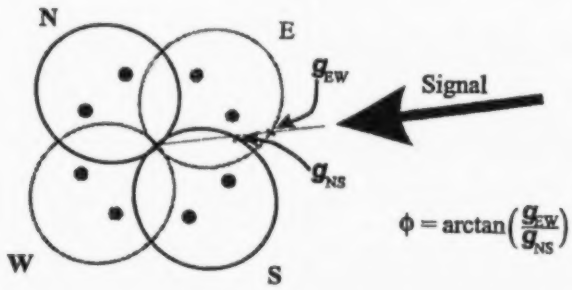

Figure 5: Antenna patterns for an eight-element circular array implementing the Watson-Watt approach.

The next two sections discuss the implementation of the Watson-Watt approach using four and eight-element circular arrays.

2.1.1 Four Element Array

Directional antennas with the sine and cosine patterns for an $N = 4$ element circular

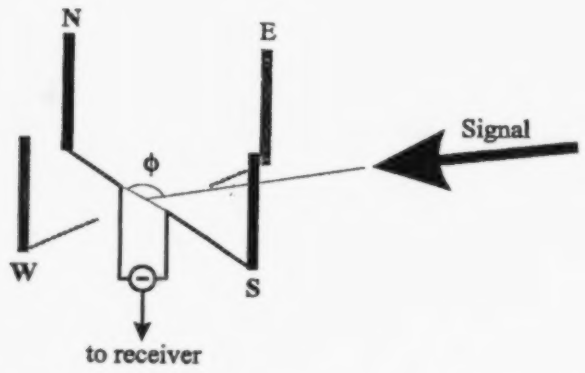

Figure 6: Adcock antenna setup for a four-element array Watson-Watt system.

array can be approximated by taking the difference in outputs from opposite pairs of antennas as shown in Figure 6 and positioning antenna 0 on the X-axis (the East-West line). Using (11) and the fact that $\vartheta = 0°$, the sine response gain pattern can be approximated by taking the difference between antennas 0 and 2 giving

$$v_{EW} = x_0 - x_2 = j2s \sin\left(\frac{2\pi r}{\lambda} \sin\phi\right) \tag{15}$$

where v_{EW} is the resultant complex voltage. The cosine response gain pattern can be generated in a similar fashion by taking the difference between antennas 1 and 3 giving

$$v_{NS} = x_1 - x_3 = j2s \sin\left(\frac{2\pi r}{\lambda} \cos\phi\right) \tag{16}$$

where v_{NS} is the resultant complex voltage.

Inspection of the above expressions reveals that for particular combinations of the bearing ϕ and array radius r, both voltages will be zero (e.g. $(\phi, r) = (0°, \lambda/2)$ or $(45°, \lambda/\sqrt{2})$). This condition can be avoided if the array radius is kept small enough that $r < r_{max_1}$ where

$$r_{max_1} = \frac{\lambda}{2} \tag{17}$$

The condition $r < r_{max_1}$ then ensures that the directional signal voltages will be nonzero regardless of the signal bearing, although for some signal bearings it will be possible to exceed this value. However, unless the reference voltage is derived from the output of a central antenna instead of using summed antenna outputs as described in Section 2.0, the actual upper limit on the array size will be $r < r_{max_0}$ (where r_{max_0} is given in (10)) since $r_{max_0} < r_{max_1}$.

Although (15) and (16) are not exactly the desired response, if the antenna array size is small enough, then the above expressions reduce to the more desirable forms

$$v_{EW} \approx j2s\frac{2\pi r}{\lambda}\sin\phi \qquad \text{for } r \ll \lambda/2\pi \tag{18}$$

and

$$v_{NS} \approx j2s\frac{2\pi r}{\lambda}\cos\phi \qquad \text{for } r \ll \lambda/2\pi \tag{19}$$

respectively.

To convert the complex voltages to more usable forms appropriate for a four quadrant arctangent function, since in most practical applications only relative phases can be measured, then the two voltages are phase shifted $-90°$ and divided by the reference voltage v_{ref} yielding

$$g'_{EW}(\phi) \;=\; -j\frac{v_{EW}}{v_{ref}} \;=\; \frac{1}{\beta}\sin\left(\frac{2\pi r}{\lambda}\sin\phi\right) \tag{20}$$

and

$$g'_{NS}(\phi) \;=\; -j\frac{v_{NS}}{v_{ref}} \;=\; \frac{1}{\beta}\sin\left(\frac{2\pi r}{\lambda}\cos\phi\right) \tag{21}$$

Provided that $r < \lambda/2\sqrt{2}$ then the term β will always be positive and real, and $g'_{EW}(\phi)$ and $g'_{NS}(\phi)$ can be used to replace $g_{EW}(\phi)$ and $g_{NS}(\phi)$ respectively, in (14). Hence

$$\hat{\phi} \;=\; \arctan\left(\frac{\sin\left(\frac{2\pi r}{\lambda}\sin\phi\right)}{\sin\left(\frac{2\pi r}{\lambda}\cos\phi\right)}\right) \tag{22}$$

The approximations (15) and (16) used for the cosine patterns lead to bias errors which are a function of both signal direction and antenna array size as shown in Figure 7. As noted already, as the antenna array size shrinks, the approximations improve and the bias error is reduced. Since the bias errors are constant and repeatable, a look-up table can be used to correct the results with relatively little processing overhead.

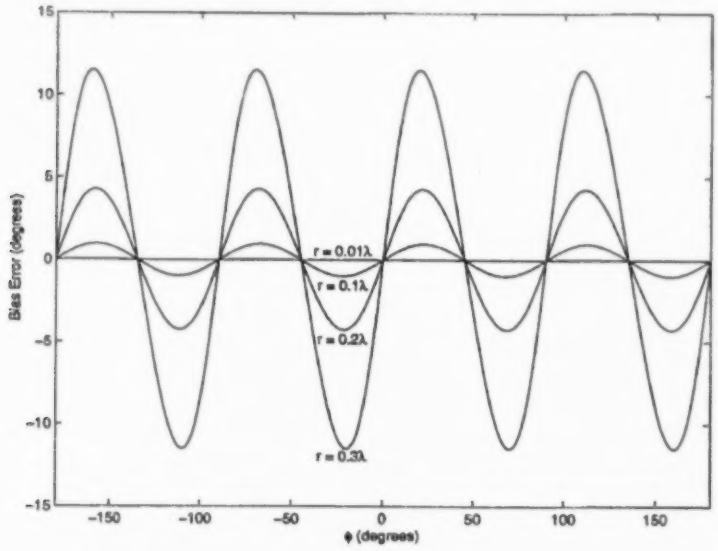

Figure 7: Bias errors of a Watson-Watt system using a four-element array showing errors as a function of the radius of the antenna array and the signal bearing.

2.1.2 Eight Element Array

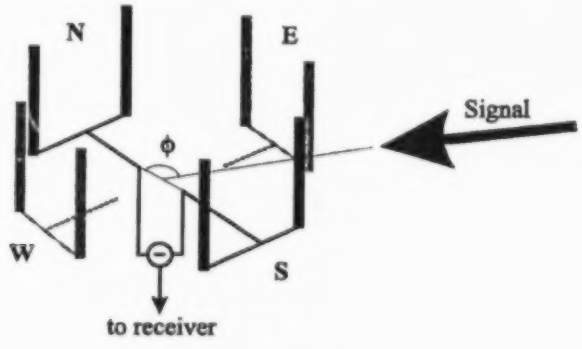

Figure 8: Adcock antenna setup for an eight-element array Watson-Watt system.

Directional antennas with the sine and cosine patterns for an $N = 8$ element circular array can be approximated by adding adjacent pairs of antennas and taking the difference in outputs between these antennas and their opposite counterparts. To properly align these patterns with the X and Y axes, the array is oriented so $\vartheta = -\pi/8$ (this aligns the long axis of rectangle formed using antennas 0, 1, 4, and 5 with the X-axis). The resultant

voltage outputs in this case are given by

$$\begin{aligned} v_{EW} &= (x_0 + x_1) - (x_4 + x_5) \\ &= j2s\sin\left(\frac{2\pi r}{\lambda}\sin(\phi - \frac{\pi}{8})\right) + j2s\sin\left(\frac{2\pi r}{\lambda}\sin(\phi + \frac{\pi}{8})\right) \qquad (23) \\ &\approx js\frac{8\pi r}{\lambda}\cos(\frac{\pi}{8})\sin\phi \qquad \text{for } r \ll \lambda/2\pi \qquad (24) \end{aligned}$$

and

$$\begin{aligned} v_{NS} &= (x_2 + x_3) - (x_6 + x_7) \\ &= j2s\sin\left(\frac{2\pi r}{\lambda}\cos(\phi - \frac{\pi}{8})\right) + j2s\sin\left(\frac{2\pi r}{\lambda}\cos(\phi + \frac{\pi}{8})\right) \qquad (25) \\ &\approx js\frac{8\pi r}{\lambda}\cos(\frac{\pi}{8})\cos\phi \qquad \text{for } r \ll \lambda/2\pi \qquad (26) \end{aligned}$$

where $\vartheta = \pi/8$ was used to adjust the array so that the long side of the rectangle formed using antennas 0, 1, 4, and 5 was aligned with the X-axis (which also aligns the resultant sine and cosine voltage patterns in the proper directions).

As in the four-element case, certain combinations of the signal bearing ϕ and the antenna array radius result both channel voltages becoming zero (e.g. $(\phi, r) = (0°, \lambda/2\cos\frac{\pi}{8})$ or $(45°, \lambda/\sqrt{2})$). This condition can be avoided if the array radius is kept small enough that $r < r_{max_1}$ where

$$r_{max_1} = \frac{\lambda}{2\cos\frac{\pi}{8}} \qquad (27)$$

This upper limit on the array radius is slightly larger than the upper limit given for the four-element array in (17) and applies for the case when a reference antenna is used at the center of the array. For the reference voltage generated using the summed antenna output the upper limit given by (10) is smaller and therefore applies.

Shifting the directional antenna voltages $-90°$ and dividing by the reference voltage to get the relevant gain values then

$$g'_{EW}(\phi) = -j\frac{v_{EW}}{v_{ref}} = \frac{1}{\beta}\sin\left(\frac{2\pi r}{\lambda}\sin(\phi - \frac{\pi}{8})\right) + \frac{1}{\beta}\sin\left(\frac{2\pi r}{\lambda}\sin(\phi + \frac{\pi}{8})\right) \qquad (28)$$

and

$$g'_{NS}(\phi) = -j\frac{v_{NS}}{v_{ref}} = \frac{1}{\beta}\sin\left(\frac{2\pi r}{\lambda}\cos(\phi - \frac{\pi}{8})\right) + \frac{1}{\beta}\sin\left(\frac{2\pi r}{\lambda}\cos(\phi + \frac{\pi}{8})\right) \quad (29)$$

Finally, the bearing estimate is determined using

$$\hat{\phi} = \arctan\left(\frac{g_{EW}(\phi)}{g_{NS}(\phi)}\right) \quad (30)$$

In terms of (28) and (29) the above expression is given by

$$\hat{\phi} = \arctan\left(\frac{\sin\left(\frac{2\pi r}{\lambda}\sin(\phi - \frac{\pi}{8})\right) + \sin\left(\frac{2\pi r}{\lambda}\sin(\phi + \frac{\pi}{8})\right)}{\sin\left(\frac{2\pi r}{\lambda}\cos(\phi - \frac{\pi}{8})\right) + \sin\left(\frac{2\pi r}{\lambda}\cos(\phi + \frac{\pi}{8})\right)}\right) \quad (31)$$

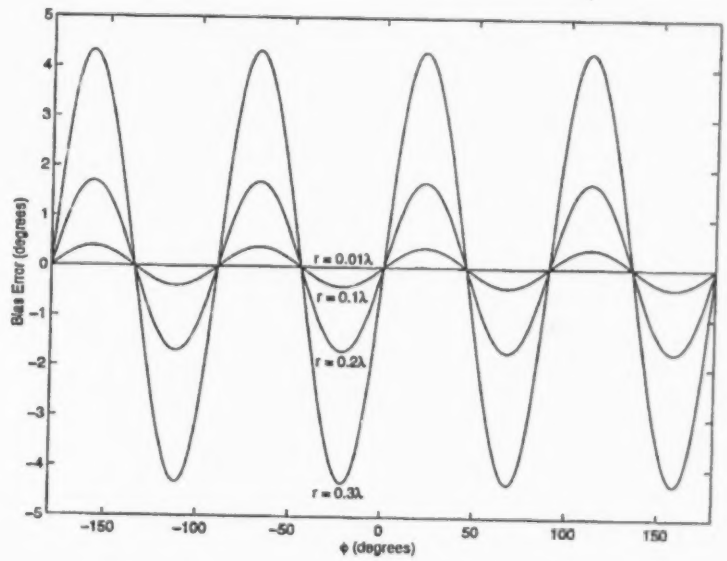

Figure 9: Bias error of a Watson-Watt system using an eight-element array as a function of the radius of the antenna array and signal bearing.

As in the four element case, the approximations (23) and (25) used for the cosine patterns lead to significant bias errors in the bearing estimates except when the array size is very small as shown in Figure 9. However the magnitude of the errors in this case are about one-third those for the four-element system. Since the bias errors are constant and repeatable, a look-up table can be used to correct the results with relatively little processing overhead.

2.2 The Butler Matrix Approach

The Butler matrix approach takes advantage of the relationship between the spatial response measured around a circular array and the signal direction. For example, the spatial phases measured around a one wavelength diameter circle for various signal bearings are shown in Figure 10 (the corresponding amplitude values are not shown since they are constant regardless of signal direction or angular position). As can be seen, the shape of the spatial response is unaffected by the signal direction, so that the signal direction can be related directly to the phase of this response waveform.

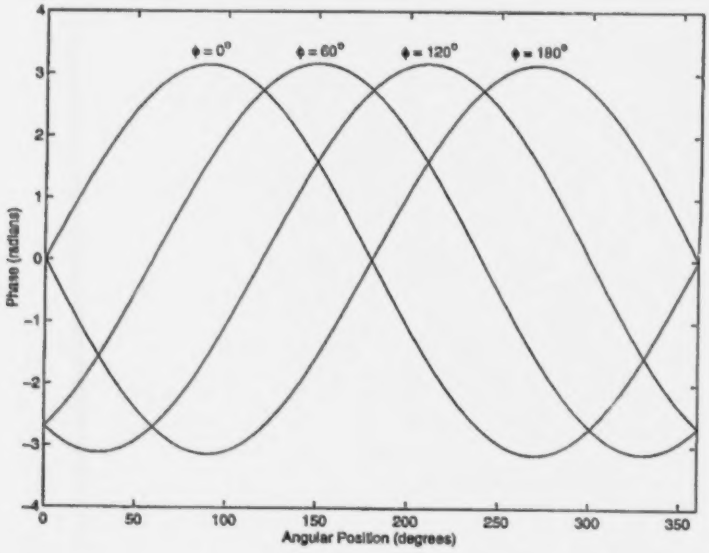

Figure 10: Spatial phase response measured around a one wavelength diameter circle for signal directions $\phi = 0°, 60°, 120°$, and $180°$. Phase measurements were made relative to the center of the circle.

Using a circular array to make discrete measurements, one method of determining the spatial phase of the response waveform is to use a Butler matrix which performs a discrete spatial Fourier transform on the data. Treating the antenna outputs as N points in a linear spatial sequence, the transform produces the sequence

$$\mathcal{F}(x_0, x_1, ...x_{N-1}) = \{f_0, f_1, ..., f_{N-1}\} \tag{32}$$

where $f_0, f_1, ..., f_{N-1}$ are the Fourier frequency coefficients. These outputs are also called the mode voltages where the mode 0 voltage is f_0, the mode 1 voltage is f_1, and so on.

The coefficients are calculated using

$$f_k = \sum_{i=0}^{N-1} x_i e^{-j\frac{2\pi ik}{N}} \tag{33}$$

Given that one complete waveform requires all N antennas, and ignoring the arbitrary phase term introduced by s, the signal modulation, then the Fourier coefficient f_1 contains the relevant spatial phase information. Since the modulation term s affects each Fourier term in the same way, its effect can be removed by dividing through by f_0. The spatial phase will then be the phase of f_1/f_0. Since the phase will change exactly as the signal direction changes, then for a suitable choice of the array orientation ($\vartheta = 0$), the phase angle and the estimated signal bearing will be the same. Hence the estimated signal bearing will be given by

$$\hat{\phi} = \arctan\left(\frac{\text{imag}\{f_1/f_0\}}{\text{real}\{f_1/f_0\}}\right) \tag{34}$$

2.2.1 Four Element Array

From (33), the mode 0 voltage f_0 is the sum of the outputs, or v_{ref}, and is calculated according to (6) where $\vartheta = 0$. The Fourier coefficient for f_1 is given by

$$\begin{aligned} f_1 &= x_0 + x_1 e^{-j\frac{\pi}{2}} + x_2 e^{-j\pi} + x_3 e^{-j\frac{3\pi}{2}} \\ &= x_0 - jx_1 - x_2 + jx_3 \\ &= (x_0 - x_2) - j(x_1 - x_3) \end{aligned} \tag{35}$$

Expanding the two bracketed terms using (11) for $n = 0$ and $n = 1$ then

$$\begin{aligned} f_1 &= j2s\sin\left(\frac{2\pi r}{\lambda}\sin\phi\right) + 2s\sin\left(\frac{2\pi r}{\lambda}\sin(\phi + \frac{\pi}{2})\right) \\ &= j2s\sin\left(\frac{2\pi r}{\lambda}\sin\phi\right) + 2s\sin\left(\frac{2\pi r}{\lambda}\cos\phi\right) \end{aligned} \tag{36}$$

Dividing this result by $f_0 = v_{ref}$, where v_{ref} is given by (6), then

$$f_1/f_0 = \frac{1}{\beta}\sin\left(\frac{2\pi r}{\lambda}\cos\phi\right) + j\frac{1}{\beta}\sin\left(\frac{2\pi r}{\lambda}\sin\phi\right) \tag{37}$$

$$\approx \frac{2\pi r}{\beta\lambda}\cos\phi + j\frac{2\pi r}{\beta\lambda}\sin\phi \qquad \text{for } r \ll \frac{\lambda}{2\pi} \tag{38}$$

Taking (37) and plugging it into (34) results in

$$\hat{\phi} = \arctan\left(\frac{\sin\left(\frac{2\pi r}{\lambda}\sin\phi\right)}{\sin\left(\frac{2\pi r}{\lambda}\cos\phi\right)}\right) \tag{39}$$

which is identical to (22), the expression developed for the Watson-Watt approach using four antennas. Hence the bias error due to approximating a continuous circle by four discrete points (i.e. using an array of four elements) is given by Figure 7.

Much like the problem of channel voltages going to zero in the Watson-Watt approach, the mode voltage f_0 and f_1 also go to zero for particular combinations of ϕ and r. The zero condition for $f_0 = v_{ref}$ was previously discussed in Section 2.0 while the zero condition for f_1 is identical to the four-element Watson-Watt approach discussed in Section 2.0 and the same limitations on array size also apply. Additionally, although a central reference antenna is not normally associated with the Butler matrix approach, this does not preclude it's use to increase the usable size of the antenna array to $r < r_{max_2}$ where $r_{max_2} = r_{max_1}$.

2.2.2 Eight Element Array

The Fourier coefficient for f_1 for an eight element array is given by

$$\begin{aligned}
f_1 &= x_0 + x_1 e^{-j\frac{\pi}{4}} + x_2 e^{-j\frac{\pi}{2}} + x_3 e^{-j\frac{3\pi}{4}} + x_4 e^{-j\pi} + x_5 e^{-j\frac{5\pi}{4}} + x_6 e^{-j\frac{3\pi}{2}} + x_7 e^{-j\frac{7\pi}{4}} \\
&= x_0 + \frac{1-j}{\sqrt{2}}x_1 - jx_2 - \frac{1+j}{\sqrt{2}}x_3 - x_4 - \frac{1-j}{\sqrt{2}}x_5 + jx_6 + \frac{1+j}{\sqrt{2}}x_7 \\
&= (x_0 - x_4) + \frac{1-j}{\sqrt{2}}(x_1 - x_5) - j(x_2 - x_6) - \frac{1+j}{\sqrt{2}}(x_3 - x_7) \\
&= (x_0 - x_4) + \frac{1}{\sqrt{2}}(x_1 - x_5) - \frac{1}{\sqrt{2}}(x_3 - x_7) \\
&\quad -j\frac{1}{\sqrt{2}}(x_1 - x_5) - j(x_2 - x_6) - j\frac{1}{\sqrt{2}}(x_3 - x_7)
\end{aligned} \tag{40}$$

Expanding the bracketed terms using (11) for $n = 0, 1, 2, 3$ and then dividing through by

$f_0 = v_{ref}$ where v_{ref} is given by (6), then

$$\begin{aligned}\text{real}\{f_1/f_0\} &= \frac{1}{\beta\sqrt{2}}\sin\left(\frac{2\pi r}{\lambda}\cos(\phi-\frac{\pi}{4})\right)+\frac{1}{\beta}\sin\left(\frac{2\pi r}{\lambda}\cos\phi\right)\\ &\quad+\frac{1}{\beta\sqrt{2}}\sin\left(\frac{2\pi r}{\lambda}\cos(\phi+\frac{\pi}{4})\right) \qquad (41)\end{aligned}$$

$$\approx \frac{\pi r\sqrt{2}}{\lambda\beta}\cos(\phi-\frac{\pi}{4})+\frac{2\pi r}{\lambda\beta}\cos\phi+\frac{\pi r\sqrt{2}}{\lambda\beta}\cos(\phi+\frac{\pi}{4})$$

$$\approx \frac{4\pi r}{\lambda\beta}\cos\phi \qquad \text{for } r \ll \frac{\lambda}{2\pi} \qquad (42)$$

and

$$\begin{aligned}\text{imag}\{f_1/f_0\} &= \frac{1}{\beta\sqrt{2}}\sin\left(\frac{2\pi r}{\lambda}\sin(\phi-\frac{\pi}{4})\right)+\frac{1}{\beta}\sin\left(\frac{2\pi r}{\lambda}\sin\phi\right)\\ &\quad+\frac{1}{\beta\sqrt{2}}\sin\left(\frac{2\pi r}{\lambda}\sin(\phi+\frac{\pi}{4})\right) \qquad (43)\end{aligned}$$

$$\approx \frac{\pi r\sqrt{2}}{\lambda\beta}\sin(\phi-\frac{\pi}{4})+\frac{2\pi r}{\lambda\beta}\sin\phi+\frac{\pi r\sqrt{2}}{\lambda\beta}\sin(\phi+\frac{\pi}{4})$$

$$\approx \frac{4\pi r}{\lambda\beta}\sin\phi \qquad \text{for } r \ll \frac{\lambda}{2\pi} \qquad (44)$$

Substituting (41) and (43) into (34) leads to the result

$$\hat{\phi} = \arctan\left(\frac{\sin\left(\frac{2\pi r}{\lambda}\sin(\phi-\frac{\pi}{4})\right)+\sqrt{2}\sin\left(\frac{2\pi r}{\lambda}\sin\phi\right)+\sin\left(\frac{2\pi r}{\lambda}\cos(\phi+\frac{\pi}{4})\right)}{\sin\left(\frac{2\pi r}{\lambda}\cos(\phi-\frac{\pi}{4})\right)+\sqrt{2}\sin\left(\frac{2\pi r}{\lambda}\cos\phi\right)+\sin\left(\frac{2\pi r}{\lambda}\sin(\phi+\frac{\pi}{4})\right)}\right) \qquad (45)$$

which is obviously quite different than the corresponding result (31) for the Watson-Watt system. The bias error (due to discrete spatial sampling) is almost insignificant in this case as shown in Figure 11. Only the result for $r = 0.3\lambda$ was shown since for smaller values of r the biasing is even smaller.

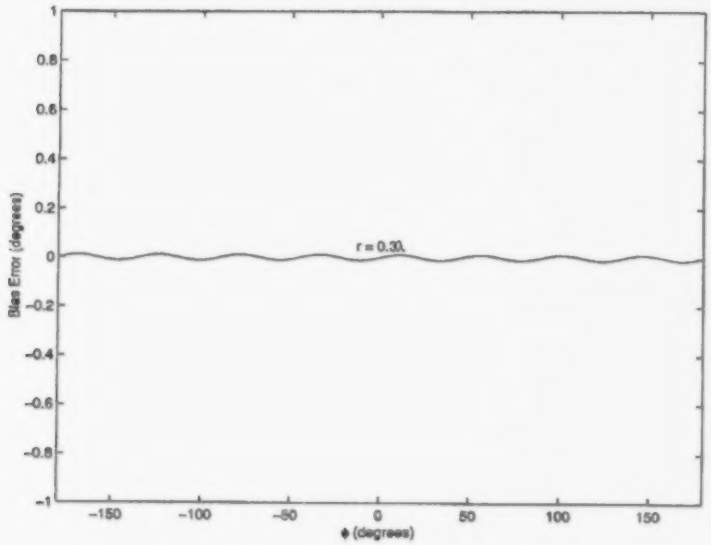

Figure 11: Bias error of a Butler matrix system using an eight-element array as a function of the signal bearing.

The problem of f_0 and f_1 going to zero for certain combinations of bearings and array sizes also affects the eight-element Butler matrix approach. The limitation on the array size based on $|f_0| = |v_{ref}| > 0$ is given by (10), while the limitation on the array size based on $|f_1| > 0$ is given by

$$r_{max_2} = 0.60564751\lambda \tag{46}$$

Since the above result is larger than given by (10), the above limit is superseded by (10). Although it would require a modification to the basic Butler matrix approach, the above limit could be reached by replacing the mode 0 output (f_0) by the output from an antenna placed at the center of the array as sometimes done for the Watson-Watt approach. If this were done, the maximum usable array size for the eight-element Butler matrix approach would then exceed that of the four-element approach as well as both the four and eight-element Watson-Watt approaches.

2.3 The Single Signal Maximum Likelihood Approach

A successful, albeit often computationally intensive and hardware expensive, approach to estimation is based on the maximum likelihood method. Essentially the idea is to find the most likely state of a signal process given a set of measurement observations made

of this process plus additive noise. Assuming the noise has a Gaussian distribution, and a measurement of N sensor outputs is available, then the associated probability density function is given by [2]

$$f(\mathbf{x}) = \frac{1}{\pi^N \det\mathbf{C}}\, e^{-\mathrm{trace}((\mathbf{x}-\mathbf{m})^H \mathbf{C}^{-1}(\mathbf{x}-\mathbf{m}))} \tag{47}$$

where the superscript H denotes the conjugate-transpose operation, $\mathbf{x}$ is the noise corrupted data vector defined by

$$\mathbf{x}_k = \begin{bmatrix} x_0 \\ x_1 \\ x_2 \\ \vdots \\ x_{N-1} \end{bmatrix} \tag{48}$$

$\mathbf{m}$ is the signal (or noise-free) data vector and has the same form as $\mathbf{x}$, and $\mathbf{C}$ is the $N \times N$ noise covariance matrix which describes the correlations among sensors. The sensor covariance matrix is assumed to be known either through measurement or modeling.

Under normal circumstances, the only unknown in (47) is the signal data vector $\mathbf{m}$. Since the Watson-Watt and Butler matrix approaches make the assumption that only a single signal is received at a particular frequency, the same assumption is made here. Hence, the elements of the signal vector $\mathbf{m}$ will be of the form

$$m_n \;=\; s e^{j\frac{2\pi r}{\lambda}\sin\left(\phi + \frac{2\pi n}{N} + \theta\right)} \qquad \text{for } n = 0, 1..., N-1 \tag{49}$$

The signal vector $\mathbf{m}$ in the single signal case is a function of the signal amplitude s and the bearing ϕ. Estimating these two values can be accomplished by finding the choice of s and ϕ which lead to a maximum value of $f(\mathbf{x})$. By inspection, this is equivalent to minimizing the expression

$$\epsilon^2 \;=\; \mathrm{trace}((\mathbf{x}-\mathbf{m})^H \mathbf{C}^{-1}(\mathbf{x}-\mathbf{m})) \;=\; (\mathbf{x}-\mathbf{m})^H \mathbf{C}^{-1}(\mathbf{x}-\mathbf{m}) \tag{50}$$

Defining the steering vector (or array response vector) as $\mathbf{e} = \mathbf{m}/(s\sqrt{N})$ and rewriting the above expression in terms of $\mathbf{e}$ then

$$\begin{aligned} \epsilon^2 \;&=\; (\mathbf{x}-s\mathbf{e})^H \mathbf{C}^{-1}(\mathbf{x}-s\mathbf{e}) \\ &=\; \mathbf{x}^H\mathbf{C}^{-1}\mathbf{x} - s\mathbf{x}^H\mathbf{C}^{-1}\mathbf{e} - s^*\mathbf{e}^H\mathbf{C}^{-1}\mathbf{x} + s^* s\mathbf{e}^H\mathbf{C}^{-1}\mathbf{e} \end{aligned} \tag{51}$$

Setting up the differential equation

$$\frac{\partial \epsilon^2}{\partial s} = 0 \tag{52}$$

yields

$$s = \frac{\mathbf{e}^H \mathbf{C}^{-1} \mathbf{x}}{\mathbf{e}^H \mathbf{C}^{-1} \mathbf{e}} \tag{53}$$

which is the value of s which minimizes ϵ^2 for a given value of ϕ. Plugging this value back into (51)

$$\epsilon^2 = \mathbf{x}^H \mathbf{C}^{-1} \mathbf{x} - \frac{\mathbf{e}^H \mathbf{C}^{-1} \mathbf{x} \mathbf{x}^H \mathbf{C}^{-1} \mathbf{e}}{\mathbf{e}^H \mathbf{C}^{-1} \mathbf{e}} \tag{54}$$

There is no obvious way to directly compute the value of ϕ, hence ϕ is estimated by finding the value which minimizes ϵ^2 using the expression shown here, or equivalently by maximizing

$$S(\phi) = \frac{\mathbf{e}^H \mathbf{C}^{-1} \mathbf{x} \mathbf{x}^H \mathbf{C}^{-1} \mathbf{e}}{\mathbf{e}^H \mathbf{C}^{-1} \mathbf{e}} \tag{55}$$

since the first term in (54) is constant with respect to ϕ.

The main advantages of the maximum likelihood (ML) approach proposed here is that it is optimum for the case of estimating the bearing of a single signal in Gaussian noise from a single measurement sample, it is also unbiased (no need for a look-up table for correction purposes), and it does not suffer from the problem of the channel voltages going to zero for certain combinations of signal bearing and antenna array size. The disadvantages are that N receiver channels are required for N antennas and it is a narrowband technique (the steering vector $\mathbf{e}$ is a function of the signal wavelength or frequency) which adds further complexity to the processing.

3.0 ERRORS DUE TO NOISE AND INTERFERENCE

In this section, the effects of internal noise, external noise, co-channel signals and multipath propagation are considered. These sources of error are grouped into two categories, namely, internal noise and external interference. To simplify the discussion, the antenna patterns are assumed to be ideal. The results derived based on these assumptions are tested later through simulation.

The approximations of interest are taken from the derivations performed previously which make the assumption that there is only one signal present and that there is no noise. The reference voltage for both the Watson-Watt and Butler approaches in this case is then given by

$$v_{ref} = as \tag{56}$$

where

$$a = 2\sum_{n=0}^{N/2-1} \cos\left(\frac{2\pi r}{\lambda}\sin(\phi + \frac{2\pi n}{N} + \vartheta)\right) = 2\beta \tag{57}$$

Although a examination of Figure 3 reveals a dependence on ϕ, for approximation purposes it is simpler to approximate β by $(\beta_{min} + \beta_{max})/2$ for the four-element array and β_{max} (where $\beta_{max} \approx \beta_{min}$) for the eight-element array. This leads to the approximation

$$a \approx \frac{N}{4}\left(1 + 2\cos\left(\frac{\pi r\sqrt{2}}{\lambda}\right) + \cos\left(\frac{2\pi r}{\lambda}\right)\right) \tag{58}$$

where $r < r_{max_0}$.

For the Watson-Watt approach the relevant channel voltage approximations are

$$v_{EW} = jbs\sin\phi \tag{59}$$

and

$$v_{NS} = jbs\cos\phi \tag{60}$$

where the best choice for b is given by

$$b = \frac{\sqrt{|v_{EW}|^2 + |v_{NS}|^2}}{|s|} \tag{61}$$

using the exact values of v_{EW} and v_{NS} described by equations (15)and (23), and equations

(16) and (25), respectively. However, this leads to a value for b which is dependent on the bearing ϕ. To remove this dependency, the median value is used instead leading to

$$b \approx \begin{cases} \sin\left(\frac{2\pi r}{\lambda}\right) + \sqrt{2}\sin\left(\frac{\pi r\sqrt{2}}{\lambda}\right) & \text{for } N = 4 \\ (2+\sqrt{2})\sin\left(\frac{2\pi r}{\lambda}\cos\frac{\pi}{8}\right) + \sqrt{2}\sin\left(\frac{2\pi r}{\lambda}\sin\frac{\pi}{8}\right) & \text{for } N = 8 \end{cases} \tag{62}$$

where $r < r_{max_1}$.

For the Butler matrix approach the relevant approximations are

$$f_0 = v_{ref} = as \tag{63}$$

and

$$f_1 = cs\cos\phi + jcs\sin\phi \tag{64}$$

where the ideal choice for c is given by

$$c = \frac{|f_1|}{|s|} = \frac{|2\beta f_1|}{|f_0|} \tag{65}$$

using the exact values of f_1/f_0 given by (37), (41), and (43) are used. Since this again results in a value which is dependent on ϕ, an approximation for c is made by taking the median value evaluated for all values of ϕ yielding

$$c \approx \begin{cases} \sin\left(\frac{2\pi r}{\lambda}\right) + \sqrt{2}\sin\left(\frac{\pi r\sqrt{2}}{\lambda}\right) & \text{for } N = 4 \\ \sqrt{2}\sin\left(\frac{\pi r\sqrt{2}}{\lambda}\right) + \sin\left(\frac{2\pi r}{\lambda}\right) + 2\cos\frac{\pi}{8}\sin\left(\frac{2\pi r}{\lambda}\cos\frac{\pi}{8}\right) & \\ \qquad + 2\sin\frac{\pi}{8}\sin\left(\frac{2\pi r}{\lambda}\sin\frac{\pi}{8}\right) & \text{for } N = 8 \end{cases} \tag{66}$$

where $r < r_{max_2}$. The expression for c for an eight-element antenna array is overly complicated and, given the range of antenna array sizes of interest, can be accurately replaced by

$$c \approx \frac{N}{4}\left(\sin\left(\frac{2\pi r}{\lambda}\right) + \sqrt{2}\sin\left(\frac{\pi r\sqrt{2}}{\lambda}\right)\right) \tag{67}$$

The main advantage of using the approximations expressed by (56), (58), (59), (60),

(62), (63), (64), and (67) is that the effects of noise and/or interference can be introduced using superposition. For example, in the case of internally generated noise plus a single interfering signal the reference voltage would be represented as

$$v_{ref} = as + as_m + n \tag{68}$$

where s_m is the complex amplitude of the interferer and n is the complex noise value. Similar modifications would also be made to (59), (60), (63), and (64).

Regardless of the conditions, the bearing for the Watson-Watt approach is estimated using

$$\hat{\phi} = \arctan\left(\frac{\text{real}\{-jv_{EW}/v_{ref}\}}{\text{real}\{-jv_{NS}/v_{ref}\}}\right) = \arctan\left(\frac{\text{real}\{-jv_{EW}\,v_{ref}^*\}}{\text{real}\{-jv_{NS}\,v_{ref}^*\}}\right) \tag{69}$$

and the bearing for the Butler matrix approach is estimated using

$$\hat{\phi} = \arctan\left(\frac{\text{imag}\{f_1/f_0\}}{\text{real}\{f_1/f_0\}}\right) = \arctan\left(\frac{\text{imag}\{f_1 f_0^*\}}{\text{real}\{f_1 f_0^*\}}\right) \tag{70}$$

For the Watson-Watt approach, in the presence of noise and/or interference the quantities v_{EW}/v_{ref} and v_{NS}/v_{ref} are no longer guaranteed to be real-valued, hence the reason for the real$\{\cdot\}$ operator.

3.1 The Effect of Internal Noise

The effect of internal noise is introduced into (56), (59), (60) (63), and (64) according to

$$v_{ref} = as + n \tag{71}$$

$$v_{EW} = jbs\sin\phi + n_{EW} \tag{72}$$

$$v_{NS} = jbs\cos\phi + n_{NS} \tag{73}$$

$$f_0 = as + n \tag{74}$$

$$f_1 = cs\cos\phi + jcs\sin\phi + n_1 \tag{75}$$

where n is the complex noise amplitude in the reference channel, n_{EW} and n_{NS} are the complex noise amplitudes in the directional channels of the Watson-Watt system, and n_1 is the complex noise amplitude of noise in the mode 1 channel of the Butler matrix system. Since each receiver channel is assumed to have the same characteristics, the RMS noise values for all channels are assumed to be the same, that is

$$E\{|n|^2\} = E\{|n_{EW}|^2\} = E\{|n_{NS}|^2\} = E\{|n_1|^2\} \tag{76}$$

3.1.1 Internal Noise and the Watson-Watt Approach

Given noise corrupted measurements of the channel voltages, the estimated signal bearing using the Watson-Watt approach is given by

$$\begin{aligned}\hat{\phi} &= \arctan\left(\frac{\text{real}\{(bs\sin\phi - jn_{EW})(as^* + n^*)\}}{\text{real}\{(bs\cos\phi - jn_{NS})(as^* + n^*)\}}\right) \\ &= \arctan\left(\frac{ab|s|^2\sin\phi + b\,\text{real}\{sn^*\}\sin\phi - \text{imag}\{as^*n_{EW} + n_{EW}n^*\}}{ab|s|^2\cos\phi + b\,\text{real}\{sn^*\}\cos\phi - \text{imag}\{as^*n_{NS} + n_{NS}n^*\}}\right)\end{aligned} \tag{77}$$

Assuming that the signal-to-noise ratio is greater than a few dB, and $a, b > 0$, then the pure noise terms in the above expression will be insignificant and the expression simplifies to

$$\hat{\phi} = \arctan\left(\frac{(|s|^2 + \text{real}\{sn^*/a\})\sin\phi - \text{imag}\{s^*n_{EW}/b\}}{(|s|^2 + \text{real}\{sn^*/a\})\cos\phi - \text{imag}\{s^*n_{NS}/b\}}\right) \tag{78}$$

The bearing error is given by $\hat{\phi} - \phi$. Taking advantage of the relationship

$$\tan(\hat{\phi} - \phi) = \frac{\tan\hat{\phi} - \tan\phi}{1 + \tan\hat{\phi}\tan\phi} \tag{79}$$

then

$$\hat{\phi} - \phi = \arctan\left(\frac{\tan\hat{\phi} - \tan\phi}{1 + \tan\hat{\phi}\tan\phi}\right) \tag{80}$$

and incorporating (78) the result (after removing any pure noise terms as was done previously) is given by

$$\hat{\phi} - \phi = \arctan\left(\frac{\text{imag}\{s^* n_{NS}/b\}\sin\phi - \text{imag}\{s^* n_{EW}/b\}\cos\phi}{|s|^2 + \text{real}\{sn^*/a\} - \text{imag}\{s^* n_{NS}/b\}\cos\phi - \text{imag}\{s^* n_{EW}/b\}\sin\phi}\right) \tag{81}$$

One last simplification can be performed by limiting the results to bearing errors of less than 10° so the approximation $\tan(\hat{\phi} - \phi) \approx \hat{\phi} - \phi$ can be used, and also by recognizing that for positive signal-to-noise ratios (particularly for levels where $\hat{\phi} - \phi < 10^\circ$) then $|s|^2 \gg \text{imag}\{s^* n/a\}\cos\phi$, $|s|^2 \gg \text{imag}\{s^* n_{NS}/b\}\cos\phi$ and $|s|^2 \gg \text{imag}\{s^* n_{EW}/b\}\sin\phi$. The appropriate simplified error expression is then given by

$$\hat{\phi} - \phi = \frac{\text{imag}\{s^* n_{NS}/b\}\sin\phi - \text{imag}\{s^* n_{EW}/b\}\cos\phi}{|s|^2} \tag{82}$$

Using the last approximation to represent the bearing error, the variance of the error can be found by taken the expectation of the squared error giving

$$\begin{aligned} E\{(\hat{\phi} - \phi)^2\} &= E\left\{\frac{(\text{imag}\{s^* n_{NS}/b\}^2 \sin\phi)^2}{|s|^4}\right\} - 2E\left\{\frac{\text{imag}\{(s^*)^2 n_{NS} n_{EW}/b^2\}\sin\phi\cos\phi}{|s|^4}\right\} \\ &\quad + E\left\{\frac{(\text{imag}\{s^* n_{EW}/b\}^2\cos\phi)^2}{|s|^4}\right\} \\ &= |s|^{-4} E\left\{\text{imag}\{s^* n_{NS}/b\}^2\right\}\sin^2\phi + |s|^{-4} E\left\{\text{imag}\{s^* n_{EW}/b\}^2\right\}\cos^2\phi \\ &= \frac{\sigma^2}{2b^2|s|^2} \end{aligned} \tag{83}$$

where it has been assumed that the signal amplitude is relatively constant, the noise is complex white Gaussian noise so that

$$E\left\{\text{imag}\{s^* n_{NS}\}^2\right\} = |s|^2 E\left\{\text{imag}\{n_{NS}\}^2\right\} = \frac{1}{2}|s|^2\sigma^2 \tag{84}$$

$$E\left\{\text{imag}\{s^* n_{EW}\}^2\right\} = |s|^2 E\left\{\text{imag}\{n_{EW}\}^2\right\} = \frac{1}{2}|s|^2\sigma^2 \tag{85}$$

and where σ^2 is the noise power.

Defining the signal-to-noise ratio as

$$snr = \frac{|s|^2}{\sigma^2} \tag{86}$$

then the RMS bearing error, which is the square-root of the variance, can be written as

$$E\{(\hat{\phi}-\phi)^2\}^{\frac{1}{2}} = \frac{1}{|b|\sqrt{2snr}} \tag{87}$$

Using the values for b defined earlier, then the RMS bearing error is given by

$$E\{(\hat{\phi}-\phi)^2\}^{\frac{1}{2}} = \begin{cases} \dfrac{1}{|\sin\left(\frac{2\pi r}{\lambda}\right) + \sqrt{2}\sin\left(\frac{\pi r\sqrt{2}}{\lambda}\right)|\sqrt{2snr}} & \text{for } N=4 \\ \dfrac{1}{|(2+\sqrt{2})\sin\left(\frac{2\pi r}{\lambda}\cos\frac{\pi}{8}\right) + \sqrt{2}\sin\left(\frac{2\pi r}{\lambda}\sin\frac{\pi}{8}\right)|\sqrt{2snr}} & \text{for } N=8 \end{cases} \tag{88}$$

The RMS bearing error expressions are somewhat complex, but for $r \ll \lambda/2\pi$ they simplify to

$$E\{(\hat{\phi}-\phi)^2\}^{\frac{1}{2}} = \begin{cases} \dfrac{\lambda}{4\pi r\sqrt{2snr}} & \text{for } N=4 \\ \dfrac{\lambda}{8\pi r\cos\frac{\pi}{8}\sqrt{2snr}} & \text{for } N=8 \end{cases} \tag{89}$$

Examining the above expressions, noise related bearing errors can be reduced by increasing the signal-to-noise ratio. Figure 12 illustrates this effect for four and eight-element arrays showing the theoretical results using (88) and the results based on computer simulations as a function of the signal-to-noise ratio defined by (86). For the simulated results, 1000 measurements for each SNR value (0 to 40 dB in 1 dB increments) were used to generate the corresponding RMS error value. Bias errors were removed before performing the RMS calculation. As can be seen, there is very good agreement between the theoretical and simulated results even for RMS errors greater than 10°. The eight-element array also has approximately half the RMS error for a given SNR than the four-element array, as predicted by (89).

The bearing errors can also be reduced by increasing the size of the array up to approximately $r = 0.3\lambda$, beyond which the error increases. This is illustrated in Figure 13 which shows the theoretical and simulated results as a function of r and three different

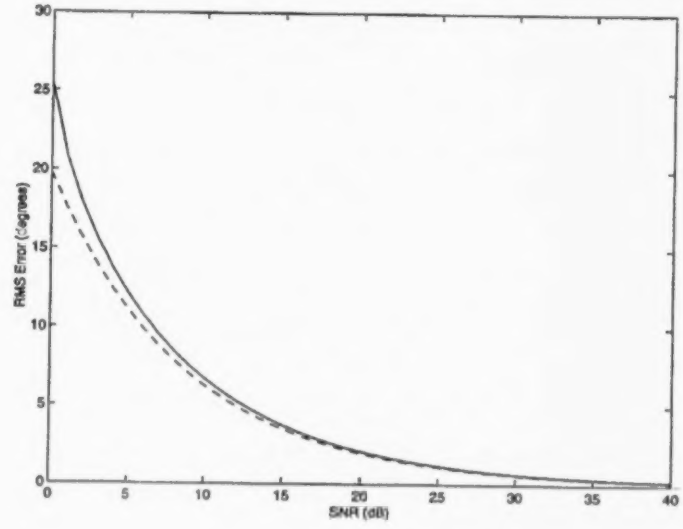

(a)

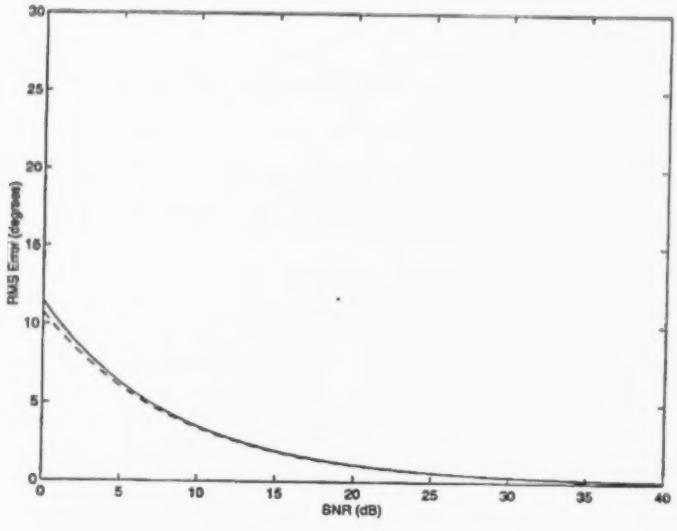

(b)

Figure 12: Effect of the internal noise level on the Watson-Watt approach using (a) a four-element and (b) an eight-element circular antenna array with a radius $r = 0.2\lambda$ and a signal bearing of $\phi = 0^{\circ}$. The simulated results are shown by the solid and the theoretical results are shown by the dashed line.

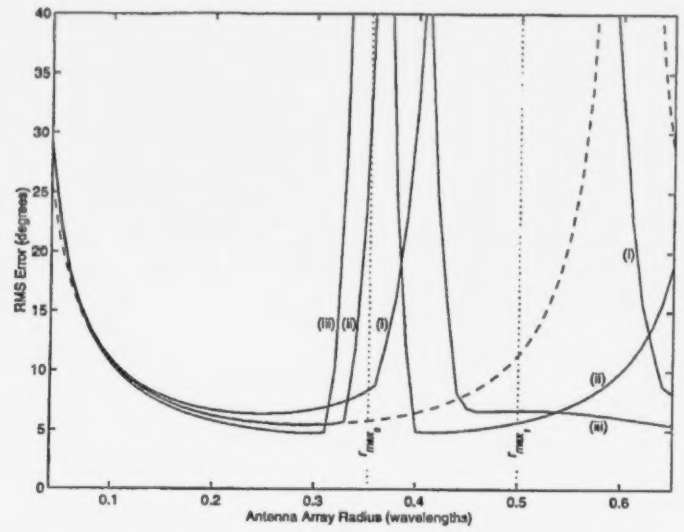

(a)

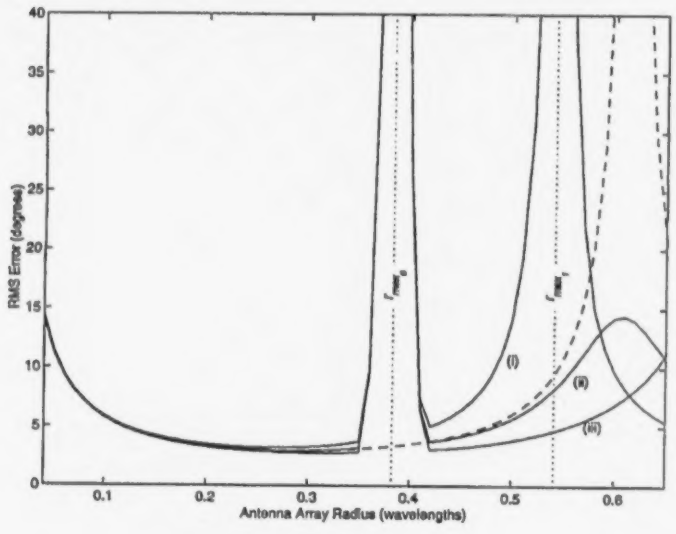

(b)

Figure 13: Effect of the antenna array radius on the Watson-Watt approach in the presence of internal noise ($snr = 10$ dB) using (a) a four-element and (b) an eight-element circular antenna array. The theoretical results are shown by the dashed line and the simulated results are shown by the solid lines for signal bearings of (i) $\phi - \vartheta = 0°$, (ii) $\phi - \vartheta = 22.5°$, and (iii) $\phi - \vartheta = 45°$.

signal angles for four and eight-element antenna arrays. For the simulated results, 1000 measurements for each value of r ranging from 0.04λ to 0.65λ in steps of 0.01λ were used to generate the corresponding RMS error values. The sign reversal in the reference channel for $r > r_{max_0}$ was corrected to yield the bearing in the correct quadrant. The simulated results illustrate that accuracy is also a function of the signal bearing. The theoretical results provide a good estimate of the median value of the RMS errors except for $r \approx r_{max_0}$ where the signal part of the reference voltage v_{ref} becomes sufficiently small that it is overpowered by noise resulting in 180° ambiguity errors (i.e. $a \to 0$ which violates the assumption made in deriving (78) and the following expressions). If a central antenna were used to measure v_{ref} then the simulated results would more closely follow the theoretical results in the region $r \approx r_{max_0}$.

3.1.2 Internal Noise and the Butler Matrix Approach

Given noise corrupted measurements of the channel voltages, the estimated signal bearing using the Butler matrix approach is given by

$$\begin{aligned}\hat{\phi} &= \arctan\left(\frac{\text{imag}\{(cs\cos\phi + jcs\sin\phi + n_1)(as^* + n^*)\}}{\text{real}\{(cs\cos\phi + jcs\sin\phi + n_1)(as^* + n^*)\}}\right) \\ &= \arctan\left(\frac{(ac|s|^2 + \text{real}\{csn^*\})\sin\phi + \text{imag}\{as^*n_1 + csn^*\cos\phi + n_1n^*\}}{(ac|s|^2 + \text{real}\{csn^*\})\cos\phi + \text{real}\{as^*n_1 + n_1n^*\} - \text{imag}\{csn^*\sin\phi\}}\right) \quad (90)\end{aligned}$$

Assuming that the signal-to-noise ratio is greater than a few dB, then the pure noise terms in the above expression will be insignificant and the expression simplifies to

$$\hat{\phi} = \arctan\left(\frac{(ac|s|^2 + \text{real}\{csn^*\})\sin\phi + \text{imag}\{as^*n_1 + csn^*\cos\phi\}}{(ac|s|^2 + \text{real}\{csn^*\})\cos\phi + \text{real}\{as^*n_1\} - \text{imag}\{csn^*\sin\phi\}}\right) \quad (91)$$

Taking advantage of the relationship expressed in (80), the bearing error can be expressed as

$$\hat{\phi} - \phi = \arctan\left(\frac{\text{imag}\{sn^*/a\} - \text{real}\{s^*n_1/c\}\sin\phi + \text{imag}\{s^*n_1/c\}\cos\phi}{|s|^2 + \text{real}\{sn^*/a\} + \text{real}\{s^*n_1/c\}\cos\phi + \text{imag}\{s^*n_1/c\}\sin\phi}\right) \quad (92)$$

where pure noise terms have again been removed.

As was done for the Watson-Watt approach, one last simplification can be performed

by limiting the results to bearing errors of less than 10° so the approximation $\tan(\hat{\phi} - \phi) \approx \hat{\phi} - \phi$ can be used, and also by recognizing that for positive signal-to-noise ratios (particularly for levels where $\hat{\phi} - \phi < 10°$) then $|s|^2 \gg |s^* n/a|^2$ and $|s|^2 \gg |s^* n_1/c|^2$. The appropriate simplified error expression is then given by

$$\hat{\phi} - \phi = \frac{\text{imag}\{sn^*/a\} - \text{real}\{s^* n_1/c\} \sin\phi + \text{imag}\{s^* n_1/c\} \cos\phi}{|s|^2} \tag{93}$$

Using the above approximation to represent the bearing error, the variance of the error can be found by taken the expectation of the squared error giving

$$\begin{aligned} E\{(\hat{\phi} - \phi)^2\} &= E\left\{\frac{\text{imag}\{sn^*/a\}^2}{|s|^4}\right\} + E\left\{\frac{\text{real}\{s^* n_1/c\}^2 \sin^2\phi}{|s|^4}\right\} \\ &\quad + E\left\{\frac{\text{imag}\{s^* n_1/c\}^2 \cos^2\phi}{|s|^4}\right\} \\ &= \frac{\sigma^2}{2|s|^2}\left(\frac{1}{a^2} + \frac{1}{c^2}\right) \end{aligned} \tag{94}$$

where it has been assumed that the signal amplitude is deterministic and the noise is complex white Gaussian in nature so that

$$E\left\{\text{imag}\{sn^*\}^2\right\} = |s|^2 E\left\{\text{imag}\{n^*\}^2\right\} = \frac{1}{2}|s|^2\sigma^2 \tag{95}$$

$$E\left\{\text{real}\{s^* n_1\}^2\right\} = |s|^2 E\left\{\text{imag}\{n_1\}^2\right\} = \frac{1}{2}|s|^2\sigma^2 \tag{96}$$

$$E\left\{\text{imag}\{s^* n_1\}^2\right\} = |s|^2 E\left\{\text{imag}\{n_1\}^2\right\} = \frac{1}{2}|s|^2\sigma^2 \tag{97}$$

and where σ^2 is the noise power.

Using the signal-to-noise ratio defined previously in (86), the RMS bearing error, which is the square root of the variance, can be written as

$$E\{(\hat{\phi} - \phi)^2\}^{\frac{1}{2}} = \sqrt{\frac{1}{2snr}\left(\frac{1}{a^2} + \frac{1}{c^2}\right)} \tag{98}$$

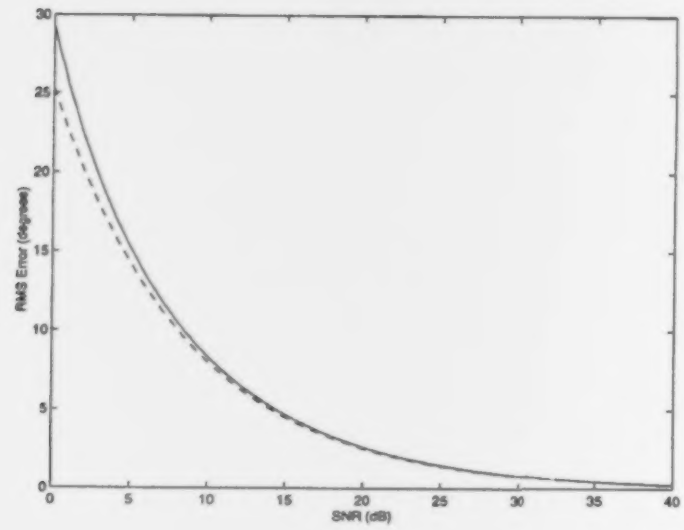

(a)

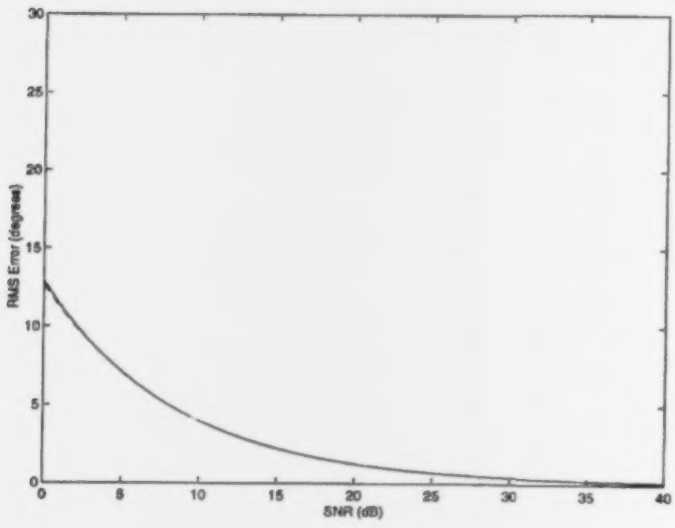

(b)

Figure 14: Effect of the internal noise level on the Butler matrix approach using (a) a four-element and (b) an eight-element circular antenna array with a radius $r = 0.2\lambda$ and a signal bearing of $\phi = 0°$. The simulated results are shown by the solid and the theoretical results are shown by the dashed line.

Applying the definition for a given by (58) and the definition for c given by (67) the RMS bearing error expression can be expanded to become

$$E\{(\hat{\phi}-\phi)^2\}^{\frac{1}{2}} = \left[\frac{8}{N^2 snr}\left(\left(1+2\cos\left(\frac{\pi r\sqrt{2}}{\lambda}\right)+\cos\left(\frac{2\pi r}{\lambda}\right)\right)^{-2} + \left(\sin\left(\frac{2\pi r}{\lambda}\right)+\sqrt{2}\sin\left(\frac{\pi r\sqrt{2}}{\lambda}\right)\right)^{-2}\right)\right]^{\frac{1}{2}} \quad (99)$$

For small array sizes where $r \ll \lambda/2\pi$ then $a \approx N$ and $c \approx N\pi r/\lambda$ and the RMS bearing error expression can also be written in a simpler form, namely,

$$E\{(\hat{\phi}-\phi)^2\}^{\frac{1}{2}} = \frac{1}{N\sqrt{2snr}}\left(1+\frac{\lambda^2}{\pi^2 r^2}\right)^{\frac{1}{2}} \quad (100)$$

Examining the RMS bearing error expression, noise related bearing errors can be reduced by increasing the signal-to-noise ratio. Figure 14 illustrates this effect for an eight-element array with $r = 0.2\lambda$ using the same data used to generate Figure 12 for the Watson-Watt approach. Bias errors were removed before performing the RMS calculation. As can be seem, there is very good agreement between the theoretical and simulated results even for RMS errors greater than 10°.

Although less obvious, the bearing errors can also be reduced by increasing the size of the array up to $r < 0.19\lambda$, beyond which the error increases substantially as noise begins to dominate the phase of the mode 0 output f_0. Since the bearing is derived from the phase of f_1/f_0, these phase errors translate directly into bearing errors. Figure 15 illustrates this effect for an eight-element array for $r \approx r_{max_0}$ using the same data that was used to generate Figure 13 for the Watson-Watt approach. The RMS errors were found to be relatively independent of direction so only one signal bearing was simulated. In theory the large errors for $r \approx r_{max_0}$ could have been eliminated by replacing the mode 0 output f_0 by the output from a central antenna. The large errors as $r \rightarrow r_{max_2}$ would be unaffected by this modification and would limit the maximum usable size of the antenna array. The agreement between the theoretical and simulated results is very good in this case.

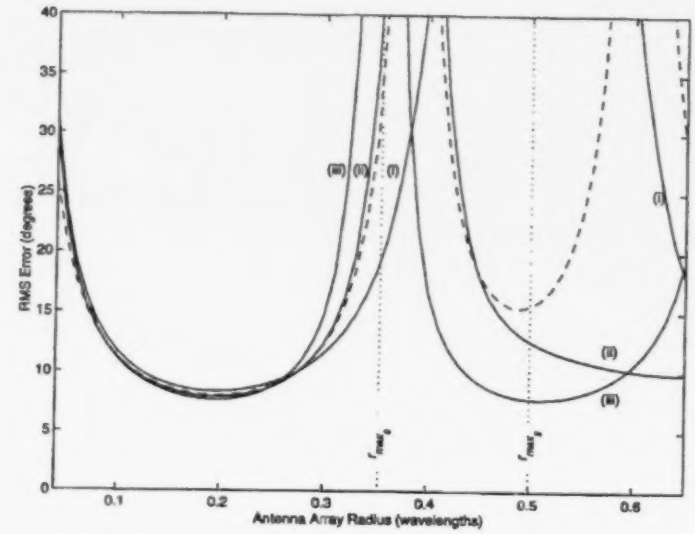

(a)

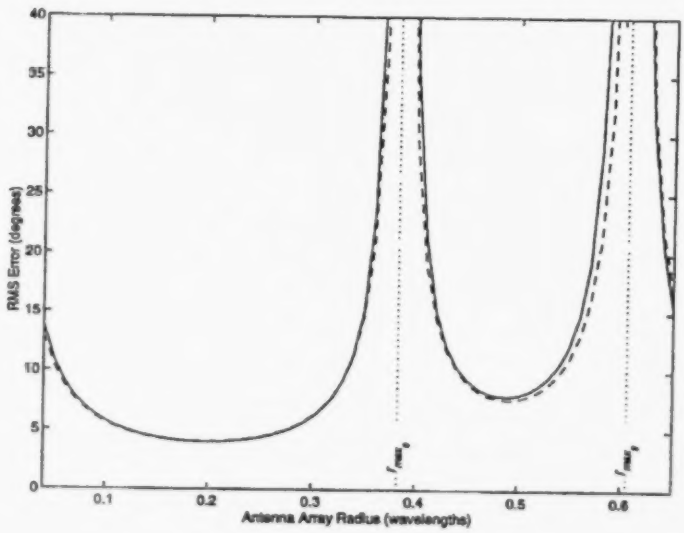

(b)

Figure 15: Effect of the antenna array radius on the Butler matrix approach in the presence of internal noise ($snr = 10$ dB) using (a) a four-element circular antenna array with signal bearings of (i) $\phi - \vartheta = 0°$, (ii) $\phi - \vartheta = 22.5°$, and (iii) $\phi - \vartheta = 45°$, and (b) an eight-element circular antenna array with a signal bearing $\phi - \vartheta = 0°$ (results for other signal bearings are the same). The theoretical results are shown by the dashed line and the simulated results are shown by the solid lines.

3.1.3 Internal Noise and Comparisons with Maximum Likelihood Performance

The performance of the Watson-Watt (worst case), Butler matrix, and ML approaches is compared in Figures 16 and 17 using the same data used to generate Figures 12 and 13 respectively. Figure 16 shows the Watson-Watt and Butler matrix results are similar and significantly better than the Maximum Likelihood approach when using an array size of $r = 0.2\lambda$. This somewhat surprising result is due to the fact that the Maximum Likelihood approach uses an eight-channel receiver with noise introduced into all eight channels. The Watson-Watt and Butler matrix approaches use a lesser number of receivers (three and two-channel receivers, respectively) resulting in a correspondingly lesser amount of noise being introduced. This, in turn, results in improved performance.

Figure 17 highlights the differences between all three approaches particularly as the radius of the array approaches $r_{max_0} = 0.35\lambda$ for the four-element array and $r_{max_0} = 0.38\lambda$ for the eight-element array. At this radius the gain of the reference channel goes to zero and the bearing estimates become extremely susceptible to noise errors. In the case of the Watson-Watt approach, the resultant phase errors only become large enough at $r = r_{max_0} - 0.03\lambda$ to cause 180° ambiguity errors which, in turn, dramatically increases the RMS bearing error level (note that for lower SNR ambiguity errors occur at a smaller value of r while for higher SNR ambiguity errors occur at a larger radius but not exceeding r_{max_0}). For the Butler matrix approach, the effect of phase errors in the reference channel is more gradual and begins at a smaller value of r so that performance is always worse than that of the Watson-Watt approach. The ML approach does not suffer zero gain problems, but for the four-element array, ambiguities in the bearing estimates occur for $r = r_{max_0}$ resulting in large bearing errors. For the eight-element array, there are no such problems so that its performance continuously improves as a function of the array radius up to $r = 0.7\lambda$ (not shown), and it also attains the lowest RMS error for $r > 0.3\lambda$ despite the extra noise.

The problem due to the reference channel could be overcome by using a dedicated antenna positioned at the center of the antenna array as mentioned previously. In the case of the Watson-Watt approach, performance would then be limited by the gain becoming too low in the two directional channels (i.e., $v_{EW}, v_{NS} \rightarrow 0$) which occurs when $r \rightarrow r_{max_1}$ (0.5λ for the four-element array and 0.54λ for the eight-element array). In the case of the Butler matrix approach, performance would be limited by the gain becoming too low in the mode 1 channel (i.e., $f_1 \rightarrow 0$) which occurs when $r \rightarrow r_{max_2}$ (0.5λ for the four-element

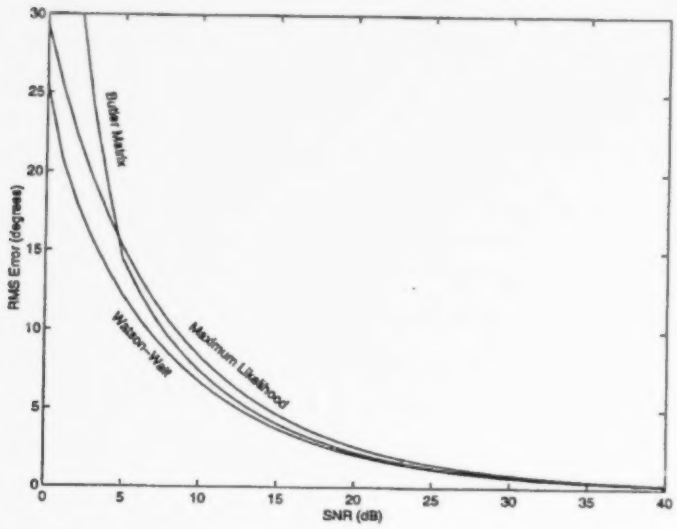

(a)

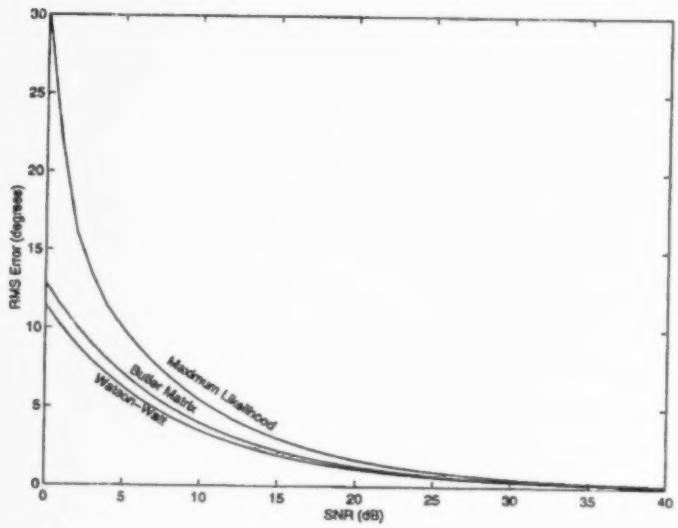

(b)

Figure 16: Effect of internal noise on the Watson-Watt, Butler matrix, and ML approaches using (a) a four-element and (b) an eight-element circular array with a radius $r = 0.2\lambda$ and a signal bearing of $\phi - \vartheta = 0^{\circ}$.

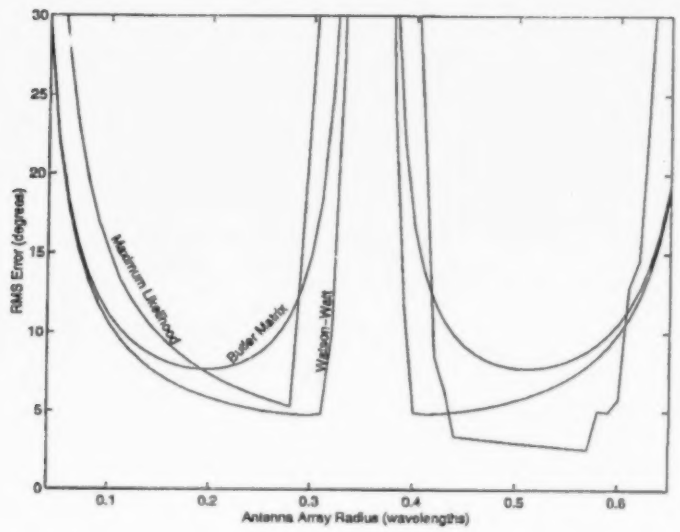

(a)

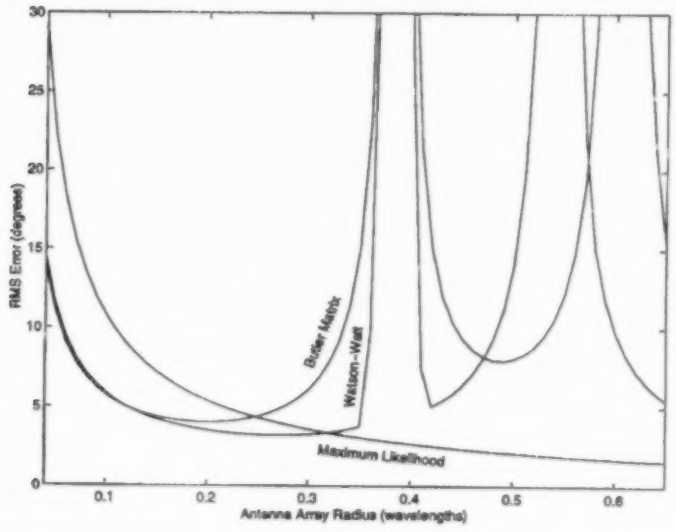

(b)

Figure 17: Effect of the antenna array radius on the performance of the Watson-Watt, Butler matrix, and ML approaches in the presence of internal noise ($snr = 10$ dB) using (a) a four-element circular array with a signal bearing of $\phi - \vartheta = 45^\circ$ and (b) an eight-element circular array with a signal bearing of $\phi - \vartheta = 0^\circ$.

array and 0.6λ for the eight-element array).

3.2 The Effect of External Interference

As mentioned previously, the term "external interference" is used to include external noise, multipath, and co-channel interference. Although these are different phenomena, they can be handled in a very similar way since they can all be modeled as a number of interfering signals. The differences in these phenomena are taken care of by adjusting the numbers of interfering signals, the statistical distribution of these signals, and their temporal and spatial correlations.

For this study, external noise was modeled as a very large number of interfering signals arriving from a wide range of directions. The advantage of this approach is that it automatically takes into account the correlations between the noise measured at different sensors – correlations which can be significant when the spacings are less than $\lambda/2$. The complex amplitudes of these signals were assumed to have a random Gaussian distribution and to be uncorrelated from measurement to measurement (temporal decorrelation), and also to be uncorrelated if the DF system was moved from site to site (spatial decorrelated). The bearings of the interfering signals were assumed to be uniformly distributed 360° in azimuth and also temporally and spatially uncorrelated. Note that this best models man-made noise which has terrestrial origins, but not isotropic or cosmic noise which has an elevation bearing component as well. The modification for isotropic noise is discussed later on.

Co-channel interference was also modeled in the same way as noise except the numbers of interfering signals were assumed to be small (i.e. one to several signals).

For modeling multipath signals, there were several key differences. The numbers of interfering signals were assumed to range from a small value for specular multipath to a large value for diffuse multipath. The complex amplitudes of these signals were assumed to have a random Gaussian distribution when measured from site to site (spatially uncorrelated), but to be invariant with time when measured for at a given site (temporally correlated). The bearings were assumed to have distributions which ranged from uniform, for sources of multipath close to the receiver, to concentrated in the direction of ϕ, for sources of multipath far from the receiver (and close to the transmitter). Other distributions are possible but were not investigated in this study. The signal bearings were also

assumed to be spatially uncorrelated but temporally correlated. The assumption of temporal correlation will not necessarily be true for all cases of multipath (e.g. HF skywave signals where path length differences can be large enough that decorrelation does occur), however the following results are not changed as long as there is either spatial or temporal decorrelation.

For any of these three types of interference, the effects of the interfering signals can be introduced into (56), (59), (60), (63), and (64) by adding the new signals according to

$$v_{ref} = a\sum_{i=0} s_i \tag{101}$$

$$v_{EW} = jb\sum_{i=0} s_i \sin\phi_i \tag{102}$$

$$v_{NS} = jb\sum_{i=0} s_i \cos\phi_i \tag{103}$$

$$f_0 = a\sum_{i=0} s_i \tag{104}$$

$$f_1 = c\sum_{i=0} s_i \cos\phi_i + js_i \sin\phi_i \tag{105}$$

where the summation limit for i is not shown but assumed to be chosen appropriate to the interference mechanism, $s_0 = s$ is the complex amplitude of the signal of interest and $\phi_0 = \phi$ is corresponding bearing (the subscript 0 was added for convenience), and $s_1, s_2, ...$ are the complex amplitudes of the interfering signals and $\phi_1, \phi_2, ...$ are the corresponding bearings.

3.2.1 Interference and the Watson-Watt Approach

Given measurements of the channel voltages corrupted by external interfering signals, the estimated signal bearing using the Watson-Watt approach is given by

$$\begin{aligned}\hat{\phi} &= \arctan\left(\frac{\text{real}\{(b\sum_{i=0} s_i \sin\phi_i)(a\sum_{i=0} s_i^*)\}}{\text{real}\{(b\sum_{i=0} s_i \cos\phi_i)(a\sum_{i=0} s_i^*)\}}\right) \\ &= \arctan\left(\frac{\sum_{i=0}\sum_{k=0}\text{real}\{s_i s_k^*\}\sin\phi_i}{\sum_{i=0}\sum_{k=0}\text{real}\{s_i s_k^*\}\cos\phi_i}\right)\end{aligned} \tag{106}$$

where the assumption that $a, b > 0$ has been made. Using the relationship expressed in (80), and after some rearranging the bearing error can be expressed as

$$\hat{\phi} - \phi = \arctan\left(\frac{\sum_{i=0}\sum_{k=0}\text{real}\{s_i s_k^*\}\sin(\phi_i - \phi_0)}{\sum_{i=0}\sum_{k=0}\text{real}\{s_i s_k^*\}\cos(\phi_i - \phi_0)}\right) \tag{107}$$

Limiting the results to bearing errors of less than 10°, then the approximation $\tan(\hat{\phi}-\phi) \approx \hat{\phi} - \phi$ will be sufficiently accurate for the purposes here. Additionally, in order for the 10° limit to be true then $|s_0| \gg |s_i|$ for $i = 1, 2, ...$ which leads to the simplified expression

$$\hat{\phi} - \phi = \frac{\sum_{i=1}\text{real}\{s_i s_0^*\}\sin(\phi_i - \phi_0)}{|s_0|^2} \tag{108}$$

For a specific measurement, given that the signal parameters are all known, then (108) can be used to determine the expected bearing error. This can be useful when exploring specific effects of co-channel interference or multipath through computer simulation. In most real-life applications, however, the signal parameters will not be known so it is of more interest to statistically quantify the errors. The most useful quantity in this regards is the RMS value. In the following derivation of the RMS value, the statistical results are based on measurements taken at different time instances and different measurement sites (while keeping the parameters of the signal of interest fixed), hence the temporal and/or spatial decorrelation properties of the interfering signal parameters can be utilized.

The RMS value can be determined by first finding the variance of the error which is given by

$$\begin{aligned} E\{(\hat{\phi} - \phi)^2\} &= E\left\{\frac{(\sum_{i=1}\text{real}\{s_i s_0^*\}\sin(\phi_i - \phi_0))^2}{|s_0|^4}\right\} \\ &= \frac{E\left\{\sum_{i=1}\text{real}\{s_i s_0^*\}^2\sin^2(\phi_i - \phi_0)\right\}}{|s_0|^4} \\ &= \frac{E\left\{\sum_{i=1}\text{real}\{s_i s_0^*\}^2\right\}E\left\{\sin^2(\phi_i - \phi_0)\right\}}{|s_0|^4} \\ &= \frac{\mu^2\alpha^2}{4|s|^2} \end{aligned} \tag{109}$$

where $s = s_0$, μ^2 is the total interference signal power given by $\mu^2 = |s_1|^2 + |s_2|^2 + ...$, α^2

is the interference distribution factor which will be discussed shortly, and the relationships

$$\sum_{i=1} E\left\{\text{real}\{s_i s_0^*\}^2\right\} = \frac{1}{2}|s|^2\mu^2 \tag{110}$$

and

$$E\left\{\sin^2(\phi_i - \phi_0)\right\} = \frac{\alpha^2}{2\pi}\int_0^{2\pi} \sin^2(\phi_i - \phi_0)d\phi_i + (1-\alpha^2)E\left\{\sin^2(\phi_0 - \phi_0)\right\} \tag{111}$$

$$= \frac{\alpha^2}{2} \tag{112}$$

were used. The factor α^2 depends on the angular distribution of the interference source and for a uniform distribution over 360° (represented by the first term in (111)) then $\alpha^2 = 1$, and for a tight distribution centered around ϕ (represented by the second term in (111)) then $\alpha^2 \approx 0$. For external noise and co-channel interference $\alpha^2 = 1$ can normally be assumed. For multipath, α^2 is interpreted as the power ratio between the part of the multipath generated as a uniform distribution and the total multipath power. The value is dependent on the signal environment. For example, given a large number of small (relative to the wavelength) scattering sources of multipath and a terrestrial signal path, most of the multipath is generated near the receiver (uniform distribution), near the transmitter and along the signal path (tight distribution) leading to a value $\alpha^2 \approx 0.5$ [3]. In another example, given a large number of large reflecting sources, the multipath region is much larger and more circular than the scattering case leading to a value $\alpha^2 \approx 1$ [3]. One final example is a calibrated airborne surveillance system, where most of the multipath will be produced near the transmitter resulting in a value of $\alpha^2 \approx 0$.

Finally, defining the signal-to-interference power ratio as

$$sir = \frac{|s|^2}{\mu^2} \tag{113}$$

(where *sir* is replaced by *snr* for external noise calculations) then the RMS bearing error is given by

$$E\{(\hat{\phi} - \phi)^2\}^{\frac{1}{2}} = \frac{\alpha}{2\sqrt{sir}} \tag{114}$$

An interesting feature of this expression is that unlike the expressions (88) and (99), developed to quantify the effects of internal noise, the size of the array and number of antennas are not factors, only the signal-to-interference power ratio. Additionally, these

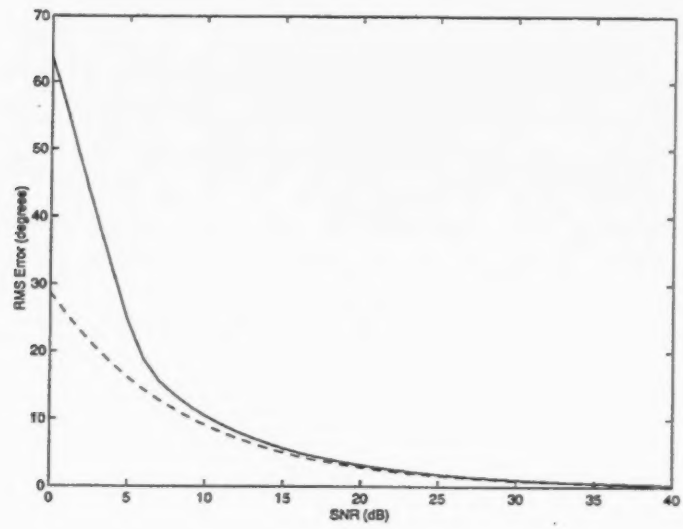

(a)

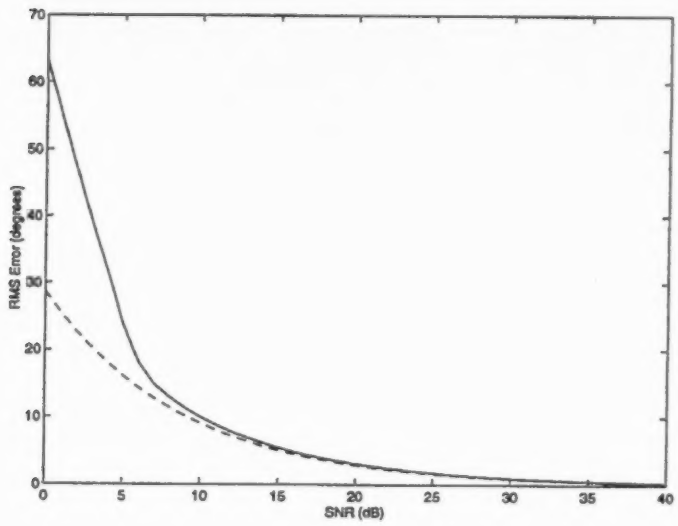

(b)

Figure 18: Effect of external terrestrial interference on a Watson-Watt system using (a) a four-element and (b) an eight-element circular antenna array with a radius $r = 0.2\lambda$ and a signal bearing $\phi = 0°$. The simulated results are shown by the solid and the theoretical results are shown by the dashed line.

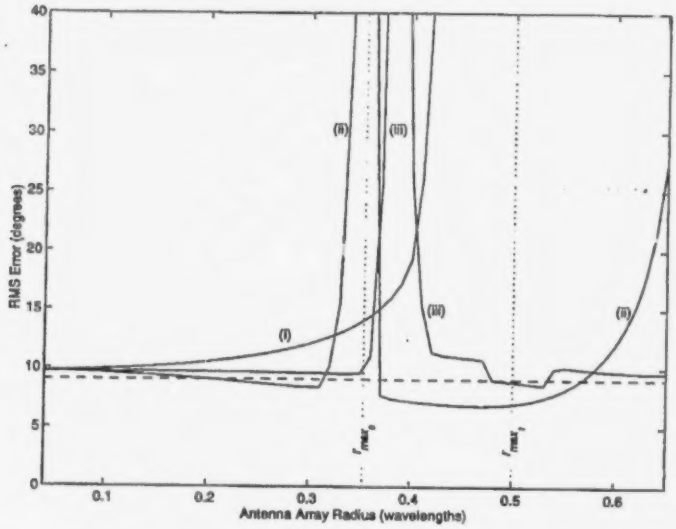

(a)

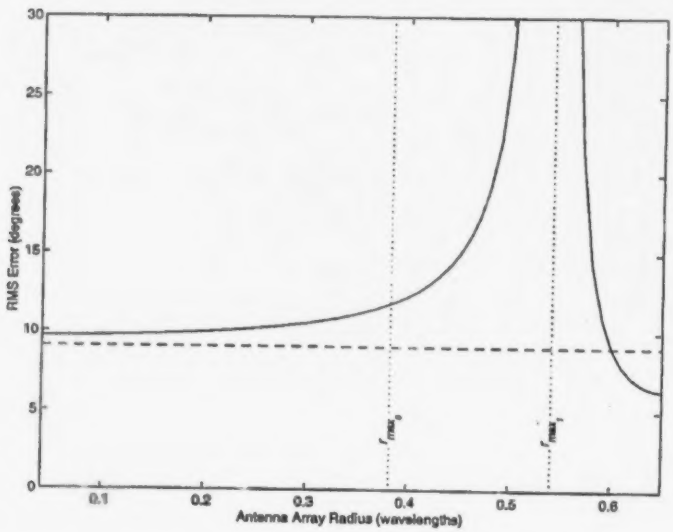

(b)

Figure 19: Effect of the antenna array radius on the Watson-Watt approach in the presence of external terrestrial interference ($sir = 10$ dB) using (a) a four-element circular antenna array with signal bearings of (i) $\phi - \vartheta = 0°$, (ii) $\phi - \vartheta = 22.5°$, and (iii) $\phi - \vartheta = 45°$, and (b) an eight-element circular antenna array with a signal bearing $\phi - \vartheta = 0°$ (results for other signal bearings are the same). The theoretical results are shown by the dashed line and the simulated results are shown by the solid lines.

expressions suggest that the low gain problem encountered in the presence of internal noise when $r \approx r_{max_0}$ or $r \approx r_{max_1}$ will not be a factor since the gain of the signal and interference will both be effected in the same way leaving the *sir* unchanged (assuming of course that internal noise is absent – an unrealistic assumption in practical applications but useful for identifying the causes of error as done here). To test these conclusions, simulations were carried out in the same way as was done for the results displayed in Figures 12 and 13) except the internal noise was replace by external terrestrial noise. The results are shown in Figures 18 and 19.

The simulated results indicate that, as predicted, the RMS errors are relatively independent of the size of the antenna array except for radii approaching the critical values $r = r_{max_0}$ and $r = r_{max_1}$. The explanation for the failure of the theoretical expressions to explain these critical array radii is due to the incorrect assumption that the appropriate channel gains go to zero at $r = r_{max_0}$ and $r = r_{max_1}$ for all signal directions. This is readily apparent, for example, when one considers that $v_{ref} \propto \beta$ and observes the variations in β shown as a function of signal direction in Figure 3 for a four-element antenna array. The result is that the gain for the interference arriving from bearings different from the signal will not necessarily go to zero when the signal gain does so that the *sir* decreases significantly and large errors result. The same problem occurs for $r = r_{max_1}$ for both the four and eight-element antenna arrays. An exception is for $r = r_{max_0}$ for the eight-element array since at this radius the gain of the reference channel is virtually independent of signal direction (see Figure 4) so that the simulated results are much closer to the theoretical expectations. However, even in this special case, under more realistic conditions, the effects of internal noise would certainly dominate.

The effect of isotropic noise can be easily introduced in the previous derivation by replacing every term $\sin\phi_i$ by $\sin\phi_i \cos\psi_i$, and every term $\cos\phi_i$ by $\cos\phi_i \cos\psi_i$ where ψ_i is the elevation angle and where the receive antennas are assumed to have an omnidirectional gain pattern. The signal of interest is still assumed to have no elevation so $\psi_0 = 0°$. For isotropic noise the interfering signals will be uniformly distributed over the half sphere formed by $0° \leq \phi \leq 360°$ and $0° \leq \psi \leq \psi/2$, hence (112) becomes

$$E\left\{\sin^2(\phi_i - \phi_0)\cos^2(\psi_i)\right\} = \frac{1}{2\pi}\int_0^{2\pi}\int_0^{\frac{\pi}{2}} \sin^2(\phi_i - \phi_0)\cos^3(\psi_i) d\psi_i d\phi_i$$

$$= \frac{1}{3} \qquad (115)$$

where $\alpha^2 = 1$ was used, and (114) becomes

$$E\{(\hat{\phi} - \phi)^2\}^{\frac{1}{2}} = \frac{1}{\sqrt{6snr}} \tag{116}$$

where *snr* was used instead of *sir* since noise is being discussed. Interestingly for the same SNR, isotropic noise causes less error than terrestrial noise implying that interference from high elevation angles has less effect than interference at low elevation angles. Figures 20 and 21 show the same noise effects as Figures 18 and 19 except isotropic noise was used instead and only the results for the eight-element antenna array have been shown. In comparing the results of isotropic noise to terrestrial noise, the same comments about the terrestrial noise apply here except that the zero gain problem has been exacerbated. In this case, for high elevation angle noise interference the gain does not go to zero at $r = r_{max_0}$ and $r = r_{max_1}$ and consequently a greater amount of interference is available to overpower the signal causing large errors for these critical antenna array sizes.

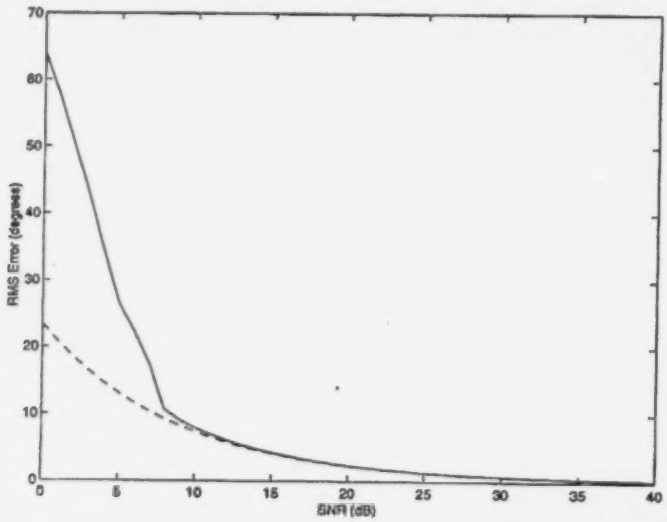

Figure 20: Effect of external isotropic noise on a Watson-Watt system using an eight-element circular antenna array with a radius $r = 0.2\lambda$. The simulated results are shown by the solid and the theoretical results are shown by the dashed line.

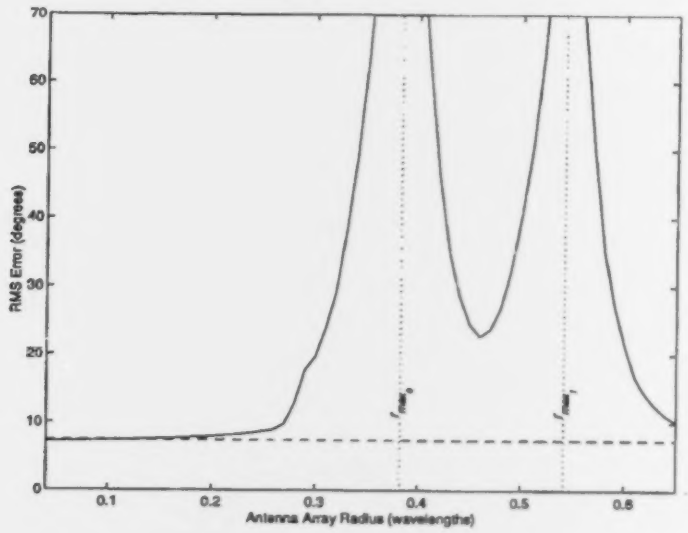

Figure 21: Effect of the antenna array radius on a Watson-Watt system using an eight-element circular antenna array in the presence of external isotropic noise ($snr = 10$ dB). The simulated results are shown by the solid and the theoretical results are shown by the dashed line.

3.2.2 Interference and the Butler Matrix Approach

Given channel voltage measurements corrupted by external interference, the estimated signal bearing using the Butler matrix approach is given by

$$\begin{aligned}\hat{\phi} &= \arctan\left(\frac{\text{imag}\{(c\sum_{i=0} s_i\cos\phi_i + js_i\sin\phi_i)(a\sum_{k=0} s_k^*)\}}{\text{real}\{(c\sum_{i=0} s_i\cos\phi_i + js_i\sin\phi_i)(a\sum_{k=0} s_k^*)\}}\right) \\ &= \arctan\left(\frac{\sum_{i=0}\sum_{k=0}\text{real}\{s_is_k^*\}\sin\phi_i + \text{imag}\{s_is_k^*\}\cos\phi_i}{\sum_{i=0}\sum_{k=0}\text{real}\{s_is_k^*\}\cos\phi_i - \text{imag}\{s_is_k^*\}\sin\phi_i}\right) \qquad (117)\end{aligned}$$

where the assumption that $a, c > 0$ has been made.

Using the relationship expressed in (80) and then rearranging, the bearing error can be expressed as

$$\hat{\phi} - \phi = \arctan\left(\frac{\sum_{i=0}\sum_{k=0}\text{real}\{s_is_k^*\}\sin(\phi_i-\phi_0) + \text{imag}\{s_is_k^*\}\cos(\phi_i-\phi_0)}{\sum_{i=0}\sum_{k=0}\text{real}\{s_is_k^*\}\cos(\phi_i-\phi_0) - \text{imag}\{s_is_k^*\}\sin(\phi_i-\phi_0)}\right) \qquad (118)$$

As has been done previously, by limiting the results to bearing errors of less than 10° then the approximation $\tan(\hat{\phi}-\phi) \approx \hat{\phi}-\phi$ can be used. Additionally, in order for the 10°

limit to be true then $|s_0| \gg |s_i|$ for $i = 1, 2, ...$, which leads to the simplified expression

$$\hat{\phi} - \phi = \frac{\sum_{i=1} \text{real}\{s_i s_0^*\} \sin(\phi_i - \phi_0) + \text{imag}\{s_i s_0^*\}(\cos(\phi_i - \phi_0) - 1)}{|s_0|^2} \tag{119}$$

Using the same line-of-reasoning to develop an RMS bearing error expression in the previous section for the Watson-Watt approach, the RMS error can be found by first determining the variance according to

$$\begin{aligned} E\{(\hat{\phi} - \phi)^2\} &= E\left\{ \frac{(\sum_{i=1} \text{real}\{s_i s_0^*\} \sin(\phi_i - \phi_0) + \text{imag}\{s_i s_0^*\}(\cos(\phi_i - \phi_0) - 1))^2}{|s|^4} \right\} \\ &= \frac{E\left\{ \sum_{i=1} \text{real}\{s_i s_0^*\}^2 \sin^2(\phi_i - \phi_0) + \text{imag}\{s_i s_0^*\}^2 (\cos(\phi_i - \phi_0) - 1)^2 \right\}}{|s|^4} \\ &= \frac{\sigma^2}{|s|^2} \end{aligned} \tag{120}$$

where the relationships in (110) and (112) were used, as well as

$$\sum_{i=1} E\left\{ \text{imag}\{s_i s_0^*\}^2 \right\} = \frac{1}{2} |s|^2 \sigma^2 \tag{121}$$

and

$$\begin{aligned} E\left\{ (\cos(\phi_i - \phi_0) - 1)^2 \right\} &= \frac{\alpha^2}{2\pi} \int_0^{2\pi} (\cos(\phi_i - \phi_0) - 1)^2 d\phi_i \\ &\quad + (1 - \alpha^2) E\left\{ (\cos(\phi_0 - \phi_0) - 1)^2 \right\} \end{aligned} \tag{122}$$

$$= \frac{3\alpha^2}{2} \tag{123}$$

and where α^2 is the angular distribution factor for multipath interference discussed in the previous section. For noise and co-channel interference $\alpha^2 = 1$.

Finally, using the definition for the signal-to-interference power ratio given earlier in (113), the RMS bearing error is given by

$$E\{(\hat{\phi} - \phi)^2\}^{\frac{1}{2}} = \frac{\alpha}{\sqrt{sir}} \tag{124}$$

As in the case of (114), the expression for Watson-Watt approach, external interference

(noise, co-channel interference, or multipath) induced bearing errors are reduced by increasing the signal-to-interference power ratio, but are unaffected by the size of the array. The RMS bearing error for the Butler matrix approach, however, is twice that for the Watson-Watt approach. This is a consequence of the fact that accurate quadrature separation of the $\cos\phi$ and $\sin\phi$ spatial signal components in the f_1 channel is dependent on the phase accuracy of the reference (f_0) channel. Any phase errors in f_0 translate directly into bearing errors. In the Watson-Watt approach the reference channel is only used to resolve 180° bearing ambiguities and bearing errors are only introduced when gross phase errors in the reference channel occur.

A comparison between the theoretical and simulated results is shown in Figures 22 and 23. The data was produced in the same manner as the data used for Figures 18 and 19. Since the qualitative similarities and differences between the simulated and predicted results are nearly identical to those for the Watson-Watt approach in Figures 18 and 19, see the discussion in the previous section.

The effect of isotropic noise can be introduced into the previous derivation by replacing every term $\sin\phi_i$ by $\sin\phi_i\cos\psi_i$, and every term $\cos\phi_i$ by $\cos\phi_i\cos\psi_i$ where ψ_i is the elevation angle and where the receive antennas are assumed to be omnidirectional. The signal of interest is still assumed to have no elevation so $\psi_0 = 0°$. For isotropic noise the interfering signals will be uniformly distributed over the half sphere formed by $0° \leq \phi \leq 360°$ and $0° \leq \psi \leq \psi/2$, hence (112) becomes

$$E\left\{(\cos(\phi_i-\phi_0)\cos(\psi_i)-1)^2\right\} = \frac{1}{2\pi}\int_0^{2\pi}\int_0^{\frac{\pi}{2}}(\cos(\phi_i-\phi_0)\cos(\psi_i)-1)^2\cos(\psi_i)d\psi_i d\phi_i$$

$$= \frac{4}{3} \tag{125}$$

where $\alpha^2 = 1$ was used. Using the relationship in (115) as well, then (124) becomes

$$E\{(\hat{\phi}-\phi)^2\}^{\frac{1}{2}} = \sqrt{\frac{5}{6snr}} \tag{126}$$

where the term *sir* was replaced by *snr* since noise is being discussed. Inspecting (124) and (126), the change in noise distribution from zero-elevation to isotropic results in lower error, although the ratio of improvement is slightly less than for the Watson-Watt system. A comparison of the theoretical and simulated results, for the eight-element antenna array only, is provided in Figures 24 and 25 which are a repeat of Figures 22 and 23 except

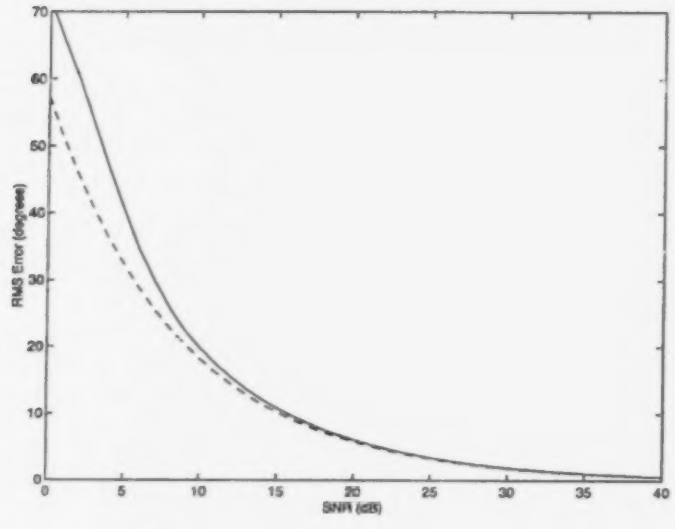

(a)

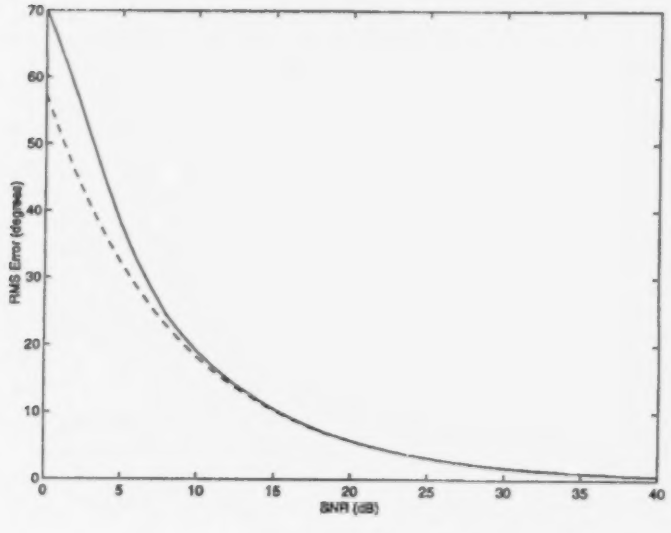

(b)

Figure 22: Effect of external terrestrial interference on a Butler matrix system using (a) a four-element and (b) an eight-element circular antenna array with a radius $r = 0.2\lambda$ and a signal bearing $\phi = 0°$. The simulated results are shown by the solid and the theoretical results are shown by the dashed line.

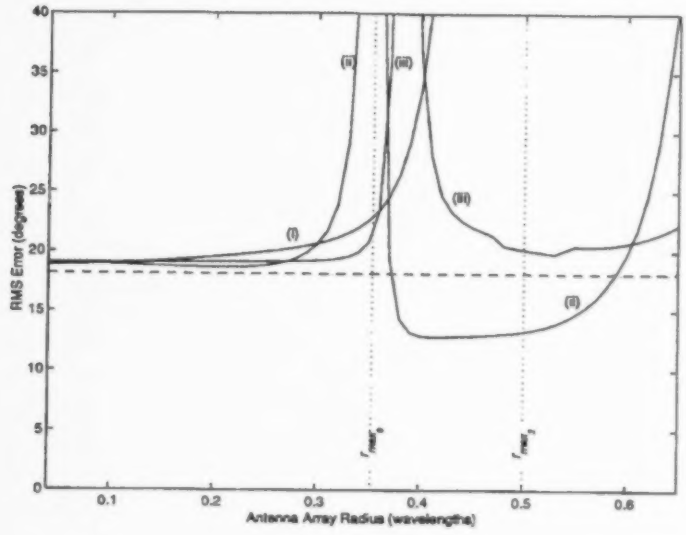

(a)

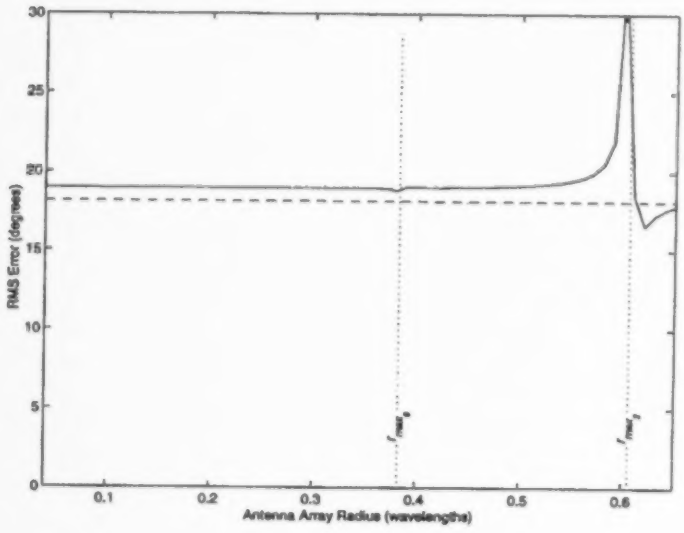

(b)

Figure 23: Effect of the antenna array radius on the Butler matrix approach in the presence of external terrestrial interference ($sir = 10$ dB) using (a) a four-element circular antenna array with signal bearings of (i) $\phi - \vartheta = 0°$, (ii) $\phi - \vartheta = 22.5°$, and (iii) $\phi - \vartheta = 45°$, and (b) an eight-element circular antenna array with a signal bearing $\phi - \vartheta = 0°$ (results for other signal bearings are the same). The theoretical results are shown by the dashed line and the simulated results are shown by the solid lines.

isotropic noise was used instead.

In comparing the results for isotropic noise to terrestrial noise, the same comments about the terrestrial noise apply here except that the zero gain problem, like the Watson-Watt approach, has been exacerbated. The gain for high elevation angle noise interference does not go to zero at $r = r_{max_0}$ and $r = r_{max_1}$ and consequently a greater amount of interference is available to overpower the signal causing large errors for these critical antenna array sizes.

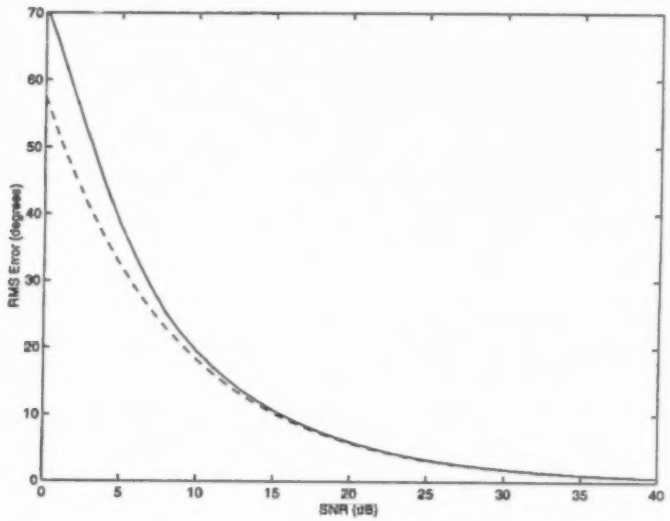

Figure 24: Effect of external isotropic noise on a Butler matrix system using an eight-element circular antenna array with a radius $r = 0.2\lambda$. The simulated results are shown by the solid and the theoretical results are shown by the dashed line.

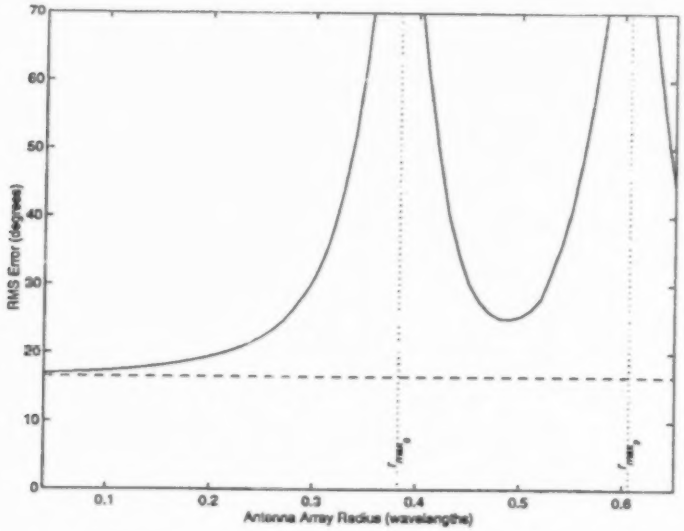

Figure 25: Effect of the antenna array radius on a Butler matrix system using an eight-element circular antenna array in the presence of external isotropic noise ($snr = 10$ dB). The simulated results are shown by the solid and the theoretical results are shown by the dashed line.

3.2.3 Interference and Comparisons with Maximum Likelihood Performance

The performance of the Watson-Watt, Butler matrix, and Maximum Likelihood approaches is compared in Figures 26-29 using the same data used to generate Figures 18-21 respectively.

Figure 26 shows performance (i.e. RMS bearing errors) as a function of the signal-to-interference ratio, and unlike the internal noise case, the ML approach significantly outperforms both the Watson-Watt and Butler matrix approaches. Increasing the number of antenna elements from four to eight also improves ML performance but has no effect on either the Watson-Watt or Butler matrix approaches. The performance of the Butler matrix suffers the most due to its increased sensitivity to phase errors in the reference channel.

Figure 27 illustrates that the performance of the Watson-Watt and Butler matrix approaches are independent of the number of antenna elements and array size for smaller arrays. Performance, however, dramatically worsens (i.e. the RMS bearing errors increase) as the array radius approaches the critical values of r_{max_0}, r_{max_1} (Watson-Watt) or r_{max_2} (Butler matrix). Outside these critical values, the Butler matrix approach is

approximately a factor of two times worse than the Watson-Watt approach. By way of comparison, the performance of the ML approach is considerably better, but it too suffers the same problems as the Watson-Watt and Butler matrix approaches when the radius approaches the critical values of r_{max_0}, r_{max_1} and r_{max_2} for the four-element array. There is no such critical radius problem for the eight-element array, however, and the ML approach works well even for array radii exceeding r_{max_2}. Overall the performance of the ML approach was a factor of two to five times better than the Watson-Watt approach, a performance improvement which can be largely attributed to the ML approach's ability to take advantage of the second order statistical nature of the noise (which is assumed to be known or measureable) as well as the advantage of using N receiver channels instead of two or three.

Figures 28 and 29 illustrate the same effects as Figures 26 and 27 except that isotropic noise was used instead and only the results for an eight element antenna array are shown. Relative performances remained unchanged and absolute performance was improved for small array sizes, but worse for an array radius approaching r_{max_0}. The poor performance for array radius values approaching r_{max_1} and r_{max_2} is unchanged from the terrestrial interference case. The performance of the ML approach was significantly better than the other two approaches and remained relatively constant for all array sizes.

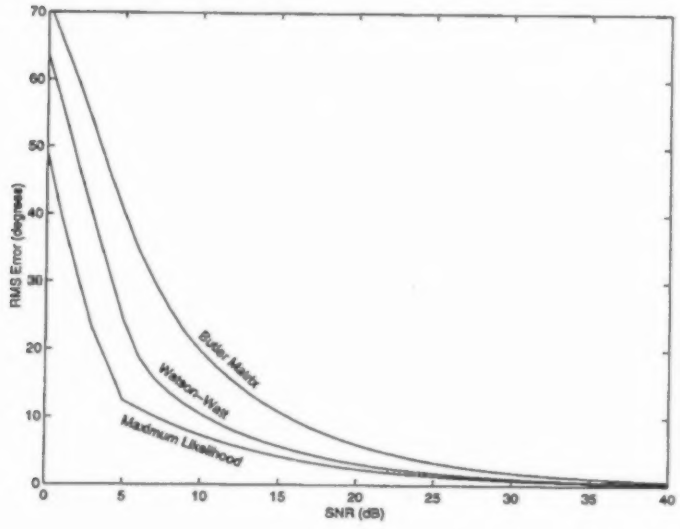

(a)

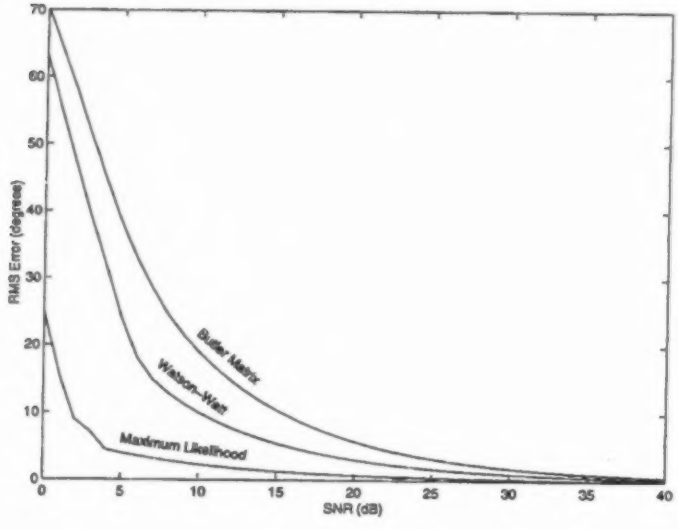

(b)

Figure 26: Effect of external noise on the Watson-Watt, Butler matrix, and ML approaches using (a) a four-element and (b) an eight-element circular array with a radius $r = 0.2\lambda$ and a signal bearing of $\phi - \vartheta = 0°$.

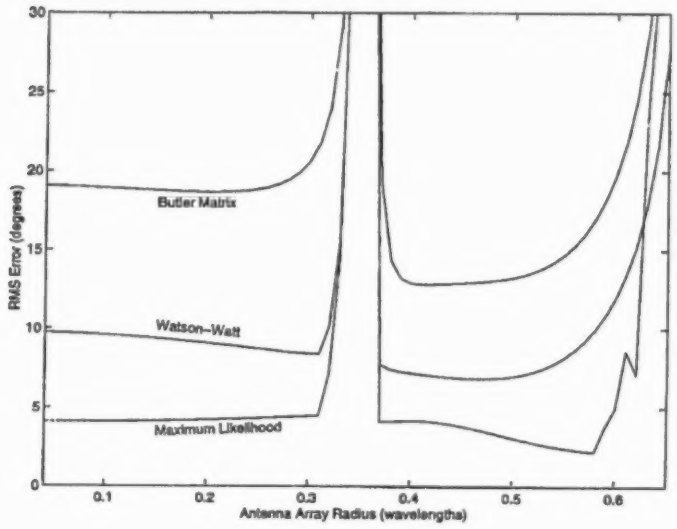

(a)

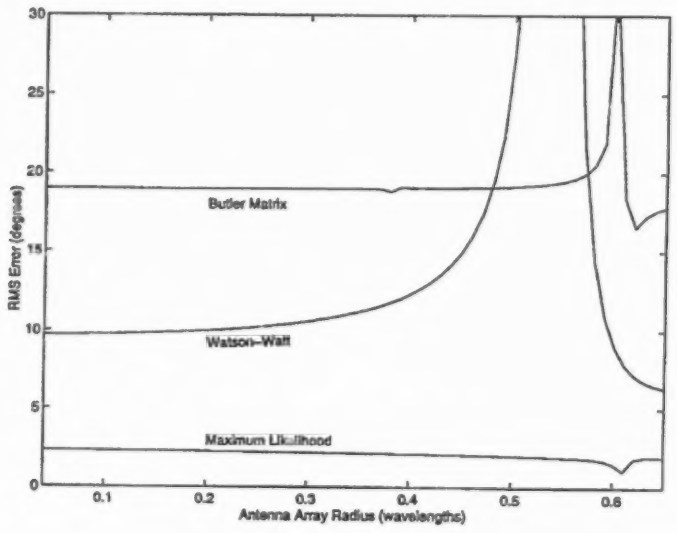

(b)

Figure 27: Effect of the antenna array radius on the performance of the Watson-Watt, Butler matrix, and ML approaches using an eight-element circular antenna array in the presence of external noise ($snr = 10$ dB) using (a) a four-element circular array with a signal bearing of $\phi - \vartheta = 45°$ and (b) an eight-element circular array with a signal bearing of $\phi - \vartheta = 0°$.

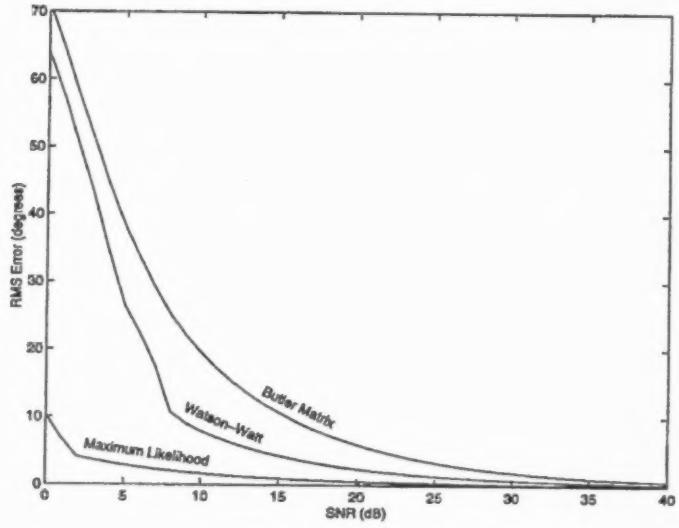

Figure 28: Effect of external isotropic noise on the Watson-Watt, Butler matrix, and ML approaches using an eight-element circular antenna array with a radius $r = 0.2\lambda$.

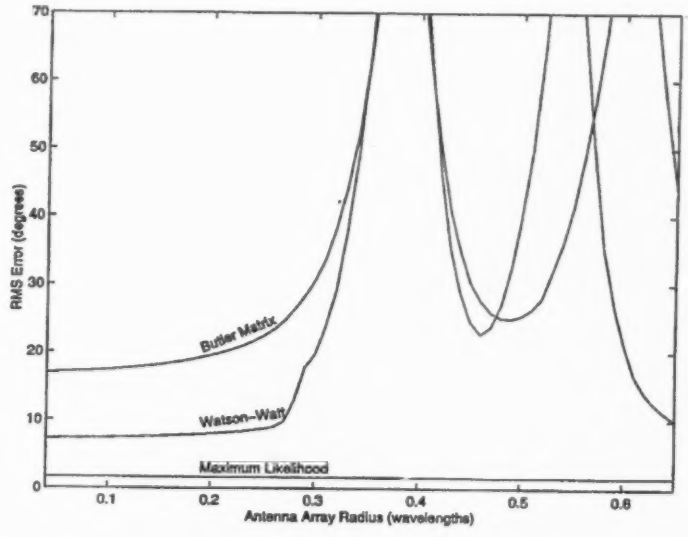

Figure 29: Effect of the antenna array radius on the performance of the Watson-Watt, Butler matrix, and ML approaches using an eight-element circular antenna array in the presence of external isotropic noise ($snr = 10$ dB).

4.0 CONCLUSIONS AND RECOMMENDATIONS

In this report, the Watson-Watt approach and Butler matrix approach – two direction finding methods developed for four and eight-element circular antenna arrays and proposed for wideband applications – were evaluated theoretically and through simulations for error causing conditions found in the real world. These conditions include internal receiver noise, external terrestrial and isotropic noise, cochannel interference and multipath. Additionally comparisons through simulation were also carried out using a maximum likelihood (ML) approach optimized for a single signal in order to determine the performance trade-off incurred using either of the two proposed wideband DF techniques. The ML approach is most closely related to correlative interferometer or vector matching approaches used in narrowband DF systems (e.g. the Watkins-Johnson 8996-1 DF processor or the Rohde & Schwarz DDF 190), the main difference being that these approaches do not compensate for the statistical distribution of noise whereas ML does.

From the implementation standpoint, the Butler matrix approach is preferable since it requires only two receiver channels compared to three receiver channels for the Watson-Watt approach. This reduces the expense in terms of wideband receivers, digitizers, etc. although some additional circuitry in the front-end is required including a quadrature mixer. By way of comparison, the ML approach would require a receiver for every antenna in the array plus a more sophisticated bearing processor owing to the greater computational complexity of this approach.

In terms of the effects of internal receiver noise, both the Watson-Watt and Butler matrix approaches had similar performance and actually outperformed the ML approach for smaller antenna arrays (i.e. less than one fifth of a wavelength) in simulations. This surprising result was due to the fact that the ML approach uses more receivers and is therefore exposed to a greater amount of noise as a result. The simulations also highlighted problems with certain antenna array sizes where channel gains of some of the channels go to zero resulting in gross bearing errors. This limits the maximum antenna array size that can be used, or equivalently, the upper frequency of the array. There is no such gain problem for the ML approach, although the four-element array suffers ambiguity problems for the same radii; the eight-element array was unaffected however.

In terms of the effect of external influences, including terrestrial or isotropic noise, cochannel interference, and multipath, the Watson-Watt approach was twice as accurate as the Butler matrix method. The main reason for the poorer accuracy of the Butler

matrix method is that errors in the reference channel, which is required for quadrature demodulation of the directional channel into its $\sin\phi$ and $\cos\phi$ bearing components, translate directly into bearing errors. In the Watson-Watt method, the $\sin\phi$ and $\cos\phi$ bearing components are contained in separate channels so that the reference channel is only required to resolve 180° bearing ambiguities.

Generally, the effect of external influences on accuracy was constant with increasing antenna array size or accuracy got worse. For the Watson-Watt and Butler matrix approaches there also appeared to be very little performance advantage in using an eight-element antenna array compared to a four-element antenna array. The problem of critical array sizes resulting in zero channel gain and causing gross bearing errors was also found to limit the usable size of the antenna array/frequency range. The ML approach was found to provide significantly better performance, particularly when using the eight element array, indicating that performance is related to the number of receiver channels used (i.e. the Butler matrix approach which used the fewest also performed the most poorly, whereas the ML approach which used the most performed the best).

For most practical applications, external influences are more likely to play a greater role in degrading DF performance than internal noise. Hence performance under these conditions is more critical in assessing the overall performance than internal noise effects (although internal noise effects cannot be ignored).

The issue of critical antenna array sizes can be broken into two problems: zero gain in the reference channel for an circular array radius of approximately $0.3 - 0.4\lambda$, and zero gain in the directional channels for a circular array radius of approximately $0.5 - 0.6\lambda$ (where λ is the signal wavelength at the desired maximum frequency). The solution to the reference channel zero gain is to use an extra antenna at the center of the antenna array rather than from the summation of the circular array antenna outputs. This could be problematic, however, if the central position is occupied by the supporting mast. There is no obvious way to deal with the zero gain problem in the directional channels so that the upper limit on circular array size is approximately $0.5 - 0.6\lambda$. The ML approach, by comparison, performs well for circular array radii up to 0.7λ without requiring an extra central antenna.

Based on these findings, the main trade-off is accuracy versus cost and speed. The ML approach achieves the highest accuracy under most conditions and has the greatest frequency range of operation. It also requires the most number of receiver channels (as many as the number of antennas) and has the greatest processing requirements making

realtime operation a much more expensive proposition. The Watson-Watt approach is less accurate, but requires only three receiver channels and has very simple processing requirements making it a much more cost effective approach. The Butler matrix approach reduces the number of receiver channels even further to two and also has simple processing requirements, but sacrifices more accuracy, having RMS bearing errors twice those of the Watson-Watt approach under practical conditions.

The conclusion is that for a system where not only accuracy, but also low cost, and realtime operation are the major requirements, the Watson-Watt approach is the best choice for current applications. In the future, however, this choice may need to be re-assessed as lower cost receivers and faster processing equipment make the ML approach a more attractive alternative.

REFERENCES

[1] Read, W.J.L., *The Effects of the Environment on an Experimental VHF Radio Direction Finding Antenna System*, DREO Report 1226, December 1994.

[2] Marple, S.L., *Digital Spectral Analysis with Applications*, Alan Oppenheim, editor, Prentice-Hall, Englewood Cliffs, New Jersey, Chapter 4, 1987.

[3] Read, W.J.L., *Multipath Modelling for Terrestrial VHF Radio Direction Finding*, DREO Report 1300, December 1996.

DOCUMENT CONTROL DATA

(Security classification of title, body of abstract and indexing annotation must be entered when the overall document is classified)

1. ORIGINATOR (the name and address of the organization preparing the document. Organizations for whom the document was prepared, e.g. Establishment sponsoring a contractor's report, or tasking agency, are entered in section 8.)

DEFENCE RESEARCH ESTABLISHMENT OTTAWA
DEPARTMENT OF NATIONAL DEFENCE
OTTAWA, ONTARIO, K1A 0Z4

2. SECURITY CLASSIFICATION (overall security classification of the document, including special warning terms if applicable)

UNCLASSIFIED

3. TITLE (the complete document title as indicated on the title page. Its classification should be indicated by the appropriate abbreviation (S,C or U) in parentheses after the title.)

AN EVALUATION OF THE WATSON-WATT AND BUTLER MATRIX APPROACHES FOR DIRECTION FINDING (U)

4. AUTHORS (Last name, first name, middle initial)

READ, WILLIAM, J.L.

5. DATE OF PUBLICATION (month and year of publication of document)

SEPTEMBER 1999

6a. NO. OF PAGES (total containing information. Include Annexes, Appendices, etc.)

59

6b. NO. OF REFS (total cited i document)

3

7. DESCRIPTIVE NOTES (the category of the document, e.g. technical report, technical note or memorandum. If appropriate, enter the type of report, e.g. interim, progress, summary, annual or final. Give the inclusive dates when a specific reporting period is covered.)

DREO Technical Report

8. SPONSORING ACTIVITY (the name of the department project office or laboratory sponsoring the research and development. Include the address.)

DEFENCE RESEARCH ESTABLISHMENT OTTAWA,
DEPARTMENT OF NATIONAL DEFENCE,
OTTAWA, ONTARIO, K1A 0Z4

9a. PROJECT OR GRANT NO. (if appropriate, the applicable research and development project or grant number under which the document was written. Please specify whether project or grant)

5BB24

9b. CONTRACT NO. (if appropriate, the applicable number under which the document was written)

10a. ORIGINATOR'S DOCUMENT NUMBER (the official document number by which the document is identified by the originating activity. This number must be unique to this document.)

DREO TR 1999-092

10b. OTHER DOCUMENT NOS. (Any other numbers which may be assigned this document either by the originator or by the sponsor)

11. DOCUMENT AVAILABILITY (any limitations on further dissemination of the document, other than those imposed by security classification)

(X) Unlimited distribution
( ) Distribution limited to defence departments and defence contractors; further distribution only as approved
( ) Distribution limited to defence departments and Canadian defence contractors; further distribution only as approved
( ) Distribution limited to government departments and agencies; further distribution only as approved
( ) Distribution limited to defence departments; further distribution only as approved
( ) Other (please specify):

12. DOCUMENT ANNOUNCEMENT (any limitation to the bibliographic announcement of this document. This will normally correspond to the Document Availability (11). However, where further distribution (beyond the audience specified in 11) is possible, a wider announcement audience may be selected.)

UNLIMITED

13. ABSTRACT (a brief and factual summary of the document. It may also appear elsewhere in the body of the document itself. It is highly desirable that the abstract of classified documents be unclassified. Each paragraph of the abstract shall begin with an indication of the security classification of the information in the paragraph (unless the document itself is unclassified) represented as (S), (C), or (U). It is not necessary to include here abstracts in both official languages unless the text is bilingual).

(U) In this report, an evaluation of the Watson-Watt and Butler matrixapproaches for tactical wideband radio direction finding applications is described. This evaluation was carried out using theoretical derivations and computer simulations, concentrating on the effects of various error mechanisms including internal noise, terrestrial and isotropic noise, cochannel interference, and multipath. A maximum likelihood (ML) approach was also derived and evaluated for comparative purposes to determine the accuracy trade-off between using an N-channel approach versus the three channel Watson-Watt approach and the two channel Butler matrix approach. The results indicate that the Watson-Watt approach is superior to the Butler matrix approach for current applications. In the future, this choice may need to be reassessed as lower cost receivers and faster processing equipment make more sophisticated approaches such as ML attractive alternatives.

14. KEYWORDS, DESCRIPTORS or IDENTIFIERS (technically meaningful terms or short phrases that characterize a document and could be helpful in cataloguing the document. They should be selected so that no security classification is required. Identifiers such as equipment model designation, trade name, military project code name, geographic location may also be included. If possible keywords should be selected from a published thesaurus. e.g. Thesaurus of Engineering and Scientific Terms (TEST) and that thesaurus-identified. If it is not possible to select indexing terms which are Unclassified, the classification of each should be indicated as with the title.)

WATSON-WATT
BUTLER MATRIX
DIRECTION FINDING
CIRCULAR ANTENNA
MAXIMUM LIKELIHOOD
RADIO FREQUENCY
NOISE
BEARING ERRORS

The Defence Research
and Development Branch
provides Science and
Technology leadership
in the advancement and
maintenance of Canada's
defence capabilities.

Leader en sciences et
technologie de la défense,
la Direction de la recherche
et du développement pour
la défense contribue
à maintenir et à
accroître les compétences
du Canada dans
ce domaine.

#512118

DEFENCE R&D DÉFENSE

www.crad.dnd.ca